Relativistic nuclear hydrodynamics and phase transition to the deconfinement state

H. W. Barz and B. Kämpfer

Central Institute of Nuclear Research, Rossendorf

B. Lukács

Central Institute of Physics Research, Budapest

Fiz. Elem. Chastits At. Yadra **18**, 1234–1282 (November–December 1987)

The possible formation of nuclear matter in the phase of a quark–gluon plasma in relativistic heavy-ion collisions is considered in the framework of a hydrodynamic approach. The main results are obtained in a single-fluid model of the formation of a baryon-enriched plasma and relate to nuclear collisions at energies up to 10 GeV/nucleon. At higher energies, a two-fluid model predicts the formation of a plasma in the fragmentation region, but the baryon density is much lower. In all the investigations, including scaling hydrodynamics in the baryon-depleted region of intermediate rapidities, allowance is made for a delayed phase transition to the deconfinement state. A generally covariant formulation of relativistic hydrodynamics is presented as a useful numerical method, together with some extensions of the methods of the standard theory (selection of comoving coordinates, allowance for sink terms, and two-fluid interaction).

INTRODUCTION

Relativistic collisions of heavy ions occur constantly when the cosmic-ray component containing heavy ions collides with nuclei in the atmosphere. The main advantage of the natural source—the high energy of the heavy ions—is not yet available to modern accelerators. The real history of relativistic heavy-ion collisions began with the systematic experimental investigations undertaken with the accelerators at Dubna (3–4 GeV/nucleon) and Berkeley ($\lesssim$2.1 GeV/nucleon) in the middle of the seventies, although a certain amount of data had been accumulated before that.

An important stimulus to the development of such experiments was the prediction of new (so-called exotic) states of nuclear matter such as a pion condensate and density isomers. These states were predicted by extrapolating certain model ideas to the region of high nuclear densities. In collisions at low and intermediate energies, one observes only a slight change in the density and low excitation energies, whereas relativistic heavy-ion collisions can lead to appreciable excitations and compressions of the nuclear matter. There is the hope that at certain sufficiently large values of the compression new forms of nuclear matter could be formed. However, it should be noted that according to the current view the conditions produced in relativistic heavy-ion collisions are not suitable for the occurrence of a pion condensate and density isomers, and this explains the failure of the experimental search for exotic signals. Although the original stimuli (or at least some of them) have not found confirmation in experiments, new ideas of scientific endeavor have arisen and generated interest among both theoreticians and experimentalists.

The main problem in this field is the description of the reaction mechanism. There is no doubt that with increasing energy of the bombarding nucleus it is necessary to go over from the average-field regime that governs the processes at low energies to the high-energy regime of two-body nucleon collisions. The mean free path of hadrons in highly excited nuclear matter, which is of the order of a few femtometers, is small compared with the spatial scale (10–15 F) of a heavy nucleus. In the general case, only a few collisions of particles are sufficient for an arbitrary distribution to approach local equilibrium. If the nucleons arrive in the state of local equilibrium sufficiently rapidly, then the relativistic heavy-ion collisions can be described by the methods of hydrodynamics. If not, one must use a kinetic, or nonequilibrium, description. At the present time, the estimate of the mean free path alone in such collisions does not yet permit us to establish which of the two regimes is realized in nature. (This, in particular, is due to the presence of a maximum for forward scattering in the interaction cross section of hadrons at relativistic energies, this hindering thermalization.) This circumstance, in conjunction with the fact that the two methods often describe the existing experimental data equally well, leads sometimes to a contrasting of hydrodynamics and a cascade. It is not our aim to discuss the essence of this contrast, but we would nevertheless like to recall the connection between kinetics and hydrodynamics.

Indeed, the possible "proximity" of relativistic heavy-ion collisions to the collective or hydrodynamic interaction regime is the most attractive feature of these processes. The hydrodynamic method makes it possible to describe the excitation of nuclear matter by means of an equation of state that can be estimated in the framework of a number of microscopic models. Since investigation of the properties of the equation of state of nuclear matter is one of the main aims of experiments on relativistic heavy-ion collisions, the hydrodynamic approach may be a suitable way of studying the dynamics of colliding nuclei. One of the most interesting questions is related to the fact that at high temperatures and densities quantum chromodynamics (QCD) predicts the existence of a new form of nuclear matter—a quark–gluon plasma. In the plasma, the quarks and gluons are no longer confined in individual nucleons. They may be liberated and travel large distances, determining thus a deconfinement region.

The idea of a change of the basic properties of hadronic

 0090-4759/87/060525-21$04.40

matter was first advanced in Ref. 1 [not on the basis of QCD but from a consideration of matter constructed from objects classified in accordance with Gell-Mann's SU(3) scheme], in Ref. 2 for cold matter in quark stars, and in Refs. 3–9, where the hot matter produced by relativistic heavy-ion collisions was considered. The last two approaches are based on the search for a region of intersection of the equations of state extrapolated from two phases: the equation of state of the hadronic phase extrapolated to the region of high densities and temperatures, and the equation of state of the plasma phase extrapolated to the region of low temperatures and densities. The presence of a point of intersection of the equations of state for these two phases is regarded as an indication of a phase transition to the deconfinement state. The only way of studying the deconfinement phase transition directly by the methods of QCD is through numerical calculations of the thermodynamic properties of quarks and gluons on a space–time lattice. The results of the lattice calculations, taken subsequently as the input data for the equation of state, must be approximated. To select a suitable approximation, one can use certain relations obtained in the two-phase model mentioned above or models that approximate by simple expressions the features of QCD calculations. Such models may be helpful in discussing variables that have not hitherto been considered in the lattice calculations because of the cumbersome nature of the calculations, for example, surface tension, which plays a central role in estimates of dynamical transitions to the deconfinement state.

If the nature of the interaction in the relativistic heavy-ion collisions is fairly close to the hydrodynamic regime, it is predicted that for energies $E \sim 10$ GeV/nucleon of the incident nuclei a short-lived plasma will be formed. The hydrodynamic description of the excitation of the plasma in such collisions is the main subject of the present review. We do not consider the experiments on relativistic heavy-ion collisions so far made (see Ref. 10). We see our aim as that of discussing future experiments on accelerators that are planned or under construction and showing what signals can be used to detect a quark–gluon plasma.

It should be noted that the best possibilities for forming a quark plasma are to be expected in ultrarelativistic collisions of heavy ions with energy $E \gtrsim 100$ GeV/nucleon. We shall briefly consider how the hydrodynamic methods can be applied to the description of collisions at such high energies. It is interesting that many of the basic ideas in this field derive from Landau's hydrodynamic model of hadron–hadron collisions.[11]

In the review, we present the basic concepts of relativistic hydrodynamics, including some of its modifications, for example, multicomponent hydrodynamics and the scheme with a sink term, and we show the possibility of including a mechanism of local relaxation for the dynamical description of the deconfinement transition. The properties of matter enter the hydrodynamics through the equation of state and the transport coefficients. We briefly discuss the equation of state and the calculation of the transport coefficients, though their derivation is outside the scope of our treatment. The central subject of discussion is the use of these methods for predicting the conditions of attainment of the deconfinement state. A general picture of the deconfinement phase transition can be obtained from the reviews of Refs. 7 and 12–14.

The main attention is devoted to a baryon-saturated plasma, i.e., $E \sim 10$ GeV/nucleon, and the fragmentation region in collisions with $E \sim 100$ GeV/nucleon.

The review is arranged as follows.

In Sec. 1, we give a consistent scheme of relativistic hydrodynamics and the connection between hydrodynamics and kinetics. In Sec. 2, we introduce a local description of matter by means of an equation of state and transport coefficients. Section 3 is devoted to a volume-averaged model for describing dynamical phase transitions. The shock-wave formalism is used in Sec. 4 to clarify the possible states of the plasma as a function of the energy of the incident nuclei ($E \sim 10$ GeV/nucleon). The part played by the delay in the appearance of the deconfinement phase in the dynamical processes is studied in Sec. 5. The main emphasis here is placed on the circumstance that the state of the plasma depends strongly on the time. The excitation of a baryon-saturated plasma in the fragmentation region of ultrarelativistic heavy-ion collisions is described in Sec. 6 in the framework of a two-fluid model, which includes effects of nuclear transparency. This section is completed by a description of the basic propositions of Bjorken's hydrodynamics for a longitudinally expanding baryon-depleted plasma in the central region of rapidities, particular attention being paid to the dynamics of the deconfinement transition. In the concluding section, we list possible signals of a plasma. Details about hydrodynamics in a comoving coordinate system, the inclusion of the charge-symmetric case, and the scheme for taking into account a sink term for continuous emission of particles can be found in the appendices.

1. BASIC HYDRODYNAMIC EQUATIONS

General equations of motion

Because of the conservation laws, or local balance with respect to the number of particles, their momentum, and energy, all forms of matter satisfy certain equations that describe the motion of the matter. The best known of these is Euler's equation for fluid dynamics.[15] We first consider the equations that control the motion of the hot compressed strongly interacting nuclear matter expected to be formed in heavy-ion collisions. Bearing in mind that in this case we are dealing with relativistic motion of matter in an exotic state, we attempt to make as few assumptions as possible concerning the particular form of the equation in which we are interested. Therefore, we begin with the most fundamental properties, gradually augmenting them by simplifying assumptions in such a way that at any stage the reason for them is clear.

In high-energy heavy-ion collisions, a fairly complicated flow pattern is expected. Therefore, the different elements of a volume of matter that are characterized by a definite energy or particle content will have very different accelerations, and if we wish to follow the development of such a collection of matter elements, it is necessary to introduce local noninertial frames of reference. This means that for the correct kinematic description it is necessary to use Riemannian geometry.[16] The four-dimensional interval between two points in a Riemannian space is defined as

$$ds^2 = g_{ij}dx^i dx^j, \tag{1}$$

where the Latin indices take the integral values 0, 1, 2, and 3,

and g_{ij} is the so-called metric tensor with signature ($-$, $+$, $+$, $+$). The distance must remain invariant on the transition from one coordinate system to another or, in other words, under any nondegenerate continuous transformation of the coordinates of the type

$$x^{i'} = x^{i'}(x^k). \tag{2}$$

The invariance of ds^2 gives the law of transformation of the metric tensor g_{ij} (here, in accordance with Einstein's rule,[16] summation is understood over all indices that appear simultaneously as subscripts and superscripts). In the absence of gravitation, space–time is a flat manifold, i.e., there exist coordinate systems for which the metric tensor has the form $g_{ij} = \mathrm{diag}(-1, +1, +1, +1)$. The condition of integrability for the existence of a transformation (2) is written as

$$R_{ijkl} = 0, \tag{3}$$

where R_{ijkl} is the Riemann tensor.[16]

The matter in space–time can be characterized by different tensors. However, one of them, the energy–momentum tensor T^{ij}, plays a distinguished role, since:

i) the balance equations for this tensor,

$$T^{ij}{}_{;j} = 0, \tag{4}$$

can be obtained from Einstein's equations of the general theory of relativity[16,17];

ii) in flat space (but for an arbitrary coordinate system) Eq. (4) enables us to construct four conserved quantities that are volume integrals of T^{ij} and can be identified with the energy and momentum[18];

iii) Eq. (4) can also be derived from the relativistic Boltzmann equation (see below).

Thus, Eq. (4) is regarded as the fundamental balance equation.

The next task is to construct a symmetric energy–momentum tensor T^{ij} for a definite form of matter. In principle, T^{ij} can be measured by observing the gravitational effects of the matter, but the practical difficulties which arise rule out this possibility. Knowing the structure of the tensor T^{ij} and the conserved quantities generated by it, we can also find its corresponding form.

Energy–momentum tensor for a rarefied gas

We consider the simplest system—a rarefied gas of (almost) point particles. Of course, it is necessary to assume the existence of some interaction between the particles, for otherwise the gas would not evolve to the equilibrium state, and this would be manifested in the form of a flow picture or a local distribution. Therefore, we assume that interaction does occur but only at very short distances. Then the life of any particle can be divided into two periods: its free motion between the remaining particles and motion in a field generated by the presence of neighboring particles. The ratio of the mean free time to the collision time can be estimated by comparing the range of the interaction with the mean free path:

$$\tau_{\mathrm{int}}/\tau_{\mathrm{free}} \sim n\sigma r_{\mathrm{int}}, \tag{5}$$

where n is the particle number density, σ is the interaction cross section, and r_{int} characterizes the interaction range. Thus, if $n\sigma r_{\mathrm{int}} \ll 1$, then the distribution function of the particles is determined primarily by the single-particle momentum distribution, whereas the relative weight of the two-particle (or higher-order) configurations will, as expected, be proportional to the ratio of the interaction times. In what follows, we shall completely ignore the correlations, describing the single-particle distribution by the relativistic Boltzmann equation[19]

$$\left(p^r \frac{\partial}{\partial x^r} - \Gamma^t_{rs} p^r p^s \frac{\partial}{\partial p^t}\right) f(p_i,\ x^k) = I(f), \tag{6}$$

where Γ^c_{ab} is the Christoffel symbol formed by the metric tensor g_{ik},[16] and it does not vanish even in the absence of gravitation if the basis is not Cartesian; f is the single-particle distribution function; and $I(f)$ is the collision integral, which describes the abrupt changes of the momentum transfer during the time of interaction at short distances. Of course, the determination of the correct form of $I(f)$ is a difficult problem. In what follows, we shall need not the specific form of $I(f)$ but rather a property that follows from the condition of conservation of the 4-momentum,

$$\int I(f)\, p^i dP = 0, \tag{7}$$

where dP denotes the infinitesimal 4-momentum volume element. If the particles are on the mass shell, then[19,20]

$$dP = d^3p/p^0. \tag{8}$$

For computational purposes, it is convenient to express $I(f)$ in the relaxation-time approximation:

$$I(f) \simeq -\frac{1}{\tau_{\mathrm{col}}}(u^r p_r)(f - f_0), \tag{9}$$

where τ_{col} is the mean time between two successive collisions of a particle, u^i is the flow velocity (sometimes expressed in terms of the mean value of the momentum; see below), and f_0 is a root of the equation $I(f) = 0$, determining the equilibrium distribution.

We now attempt to identify T with the second moments of the momentum:

$$T^{ik} = \langle p^i p^k \rangle \equiv \int f p^i p^k\, dP. \tag{10}$$

In fact, this is the only possible tensor with two indices that be constructed from quantities that characterize point particles. Then Eq. (4) must be satisfied, this being a direct consequence of (6) and (7). Thus, Eq. (10) gives an energy–momentum tensor with the required properties. Since our system is sufficiently rarefied, the gas can be regarded as a cloud of almost free particles whose behavior is controlled by the Boltzmann equation, and any quantity can be expressed in terms of the single-particle function $f(p_i, x^k)$, for example, by forming the corresponding moments (for details, see Refs. 19 and 20). However, when one attempts to apply this method to real systems, two serious problems arise:

i) the single-particle distribution function f has infinitely many degrees of freedom (more than the tensor T^{ij});

ii) for systems that are not too strongly rarefied it is necessary to take into account correlations.

The first problem is absent in the limit of thermodynamic equilibrium (or equilibrium in the momentum space). We note that the characteristic time of momentum equilibrium, i.e., of tending to f_0, is approximately equal to τ_{col}, or at least it is when other processes such as expansion of

the system do not hinder equilibrium. If τ_{col} is much less than any other time characteristic of the macroscopic behavior of the matter, for example, the change of the flow pattern, then it is reasonable to assume that

$$f = f_0, \tag{11}$$

where f_0 is determined by the gross structure of the collision integral. The particular form of $I(f)$ depends both on the differential collision cross section and on the population of the final state,[20] while f_0 is determined only by the last factor and in accordance with quantum statistics is given as

$$f_0(p_i,\ x^k) = \frac{d}{(2\pi\hbar c)^3}\left[\exp\left(\alpha + \beta u^r p_r\right) + k\right]^{-1}. \tag{12}$$

Here, α and β do not depend on p^i, although they may contain a dependence on the coordinates, d is a factor that takes into account the degeneracy with respect to the spin, isospin, etc., and, finally,

$$k = \begin{cases} +1 \text{ for Fermi statistics,} \\ 0 \text{ for Boltzmann statistics,} \\ -1 \text{ for Bose statistics.} \end{cases} \tag{13}$$

Thus, it follows from the relation (12) that the single-particle distribution function has five undetermined parameters, namely, α, β, and the three independent components u^i (because of the factor β, the 4-vector u^i can always be normalized to a unit timelike vector). These five parameters can be determined by means of five equations for the moments of the function f. Indeed, Eqs. (4) and (10) give four evolution equations. A fifth equation can be obtained by postulating the existence of a balance equation for the particle flux n, defined for particles with mass as

$$n^r{}_{;r} = \nu, \tag{14}$$

where

$$n^i = \frac{1}{m}\int f p^i\, dP, \tag{15}$$

and m is the rest mass. [For massless particles, it is necessary to give a different definition of the flux (15).] In Eq. (14), ν characterizes the source. If the interaction cross section in the collision integral $I(f)$ does not contain processes of creation, annihilation, fusion, or decay of particles, then ν is zero.[20] The equations for the divergence of T^{ij} and n^i (with a known source) now completely determine the five free parameters of the function f, and the particle number density n is given as

$$n = \sqrt{n^i n_i}, \tag{16}$$

while

$$u^i = n^i/n \tag{17}$$

is the four-dimensional velocity of the element of matter. The quantities α and β are interpreted as combinations of the ordinary thermodynamic parameters μ/T and T, as can be seen directly from Eq. (12).

Of course, there are several serious arguments in favor of Eq. (12). First, f_0 must satisfy the Liouville equation or, in other words, Eq. (6) with a vanishingly small right-hand side, for otherwise the system cannot remain in the state f_0. A necessary condition for this is an inertial nature of the motion of the fluid elements.[20] Thus, in the case of a more complicated flow pattern we will observe deviations from the form of the equilibrium momentum distribution, these being associated, for example, with transport processes (viscosity, heat conduction, diffusion, etc.)[21] or with dethermalization due to global accelerated motion of the complete system.[22] Second, even if f_0 is a solution of the Liouville equation, a system with an initial distribution far from thermodynamic equilibrium need not reach the equilibrium state if the lifetime of the system is long compared with τ_{col}. We shall see below that nonequilibrium features due to transport processes can be readily included (at least, in a certain approximation) in the approach based formally solely on f_0; in other cases, it is possible to introduce special "pseudothermodynamic" parameters.[23]

Energy–momentum tensor for homogeneous fluids

The problem of including two-particle (or higher-order) correlations is rather complicated. In principle, one could replace the Boltzmann equation by an infinite set of evolution equations for many-particle distribution functions.[24] Another possibility is to limit the set of evolution equations to

$$T^{ij}{}_{;j} = 0; \tag{18}$$

$$n^i{}_{;i} = 0, \tag{19}$$

but take into account correlations in the structure of the energy–momentum tensor. In other words, one can assume the existence of thermal equilibrium in the case when the local state is completely described by five parameters and then not calculate the tensor T^{ij} (10) in terms of the single-particle distributions. In the present paper, we follow this route.

If the many-particle distribution function $f(p_1,\ldots,p_N)$ cannot be expressed in terms of single-particle distribution functions f_0, then it is not possible to calculate T^{ij} directly. Nevertheless, even in this case the tensor T^{ij} has a definite structure, and it can be decomposed with respect to any timelike vector field u^i as

$$T^{ik} = eu^i u^k + q^i u^k + q^k u^i + P^{ik},$$
$$q_i u^i = 0,\ P_{ij}u^j = 0. \tag{20}$$

For an observer moving with velocity u^i in his own three-dimensional space, e is the energy density, q^i is the energy flux, and P_{ij} is the matter stress tensor. Now, if the state of the matter is sufficiently coherent, then there exist in the matter vector fields with respect to which the decompositions can be made. There are two obvious candidates: either the energy flow rate, defined as[15,25]

$$T^{ir}{}_{(e)}u_r = t_{(e)}u^i, \tag{21}$$

or the particle velocity

$$n^i = n_{(I)}u^i. \tag{22}$$

Choosing one of them, we go over to a comoving coordinate system, moving with the self-frame of the matter, in which the matter is in a state of rest and ordinary three-dimensional thermodynamics can be used, i.e., e, q^i, and P_{ik} can be constructed in the usual manner from n, T, and u^i. Ignoring now the transport processes (they are discussed in the following section) and assuming that the stresses are isotropic, we obtain

$$T^{ik} = eu^i u^k + P\,(g^{ik} + u^i u^k); \tag{23}$$

$$n^i = nu^i, \tag{24}$$

where P is a certain dynamical pressure. Equations (18) and (19) now take the form

$$(e + P)\,a^i = -P_{,r} g^{ir} - \dot{P}u^i; \tag{25}$$

$$\dot{e} + (e + P)\,u^r{}_{;r} = 0; \tag{26}$$

$$\dot{n} + nu^r{}_{;r} = 0, \tag{27}$$

where the acceleration is

$$a^i = u^i{}_{;r} u^r; \tag{28}$$

the dot denotes the comoving derivative with respect to the time,

$$\dot{P} = P_{,r} u^r, \tag{29}$$

and the comma denotes the partial derivative. These are the relativistic Euler equations, expressing the balance with respect to the particle number and energy. Methods of solving them are described in Appendix A. It remains to specify the connection between e, P, and n, after which Eqs. (25)–(27), which control the evolution process, will be completely determined.

For rarefied gases in the state of equilibrium, the relations (10)–(12) directly give the necessary connection in the form of the equation of state, for example, for a Boltzmann gas in the nonrelativistic limit

$$P = \frac{2}{3}(e - mn) = nT. \tag{30}$$

For an interaction with a short but finite range, the corrections to P are usually calculated by means of the virial expansion.[26] For example, strong repulsion at short distances with weak attraction at large distances leads to a van der Waals correction of the type

$$P = nT\,(1 - nV)^{-1} - bn^2, \tag{31}$$

where b and V are constant parameters of the interaction. If the interaction is strong and $n\sigma r_{\text{int}}$ is of order unity, then for such cases there is no systematic method for deriving the hydrodynamic form from the kinetic form. Nevertheless, even then Eqs. (18) and (19) must be valid, and the tensor T^{ij} has the structure given by the relation (20), so that Eqs. (25)–(27) still remain valid.

2. LOCAL DESCRIPTION OF THE MATTER

Equation of state

Thermodynamic relations

The relations (23) and (24) lead to evolution equations of the matter, although this system is not closed. It is necessary to specify the relationship between P, n, and e, which characterize the matter. We have already seen that such a connection can be obtained for an ideal gas; however, in a more general case it is not possible to guess the form of this relationship in advance. In order to avoid discussing each time each new particular example, we shall discuss this question on the basis of general thermodynamic laws.

All three considered quantities are defined in the comoving coordinate system. We now assume that the local state of the matter can be described by the methods of thermodynamics.[20,27] Then there exists a flux s^i of the entropy density. In the most general case, the tensor T^{ij} contains two independent vector fields u^i and q^i, so that s^i can be decomposed with respect to them:

$$s^i = su^i + \beta q^i, \tag{32}$$

where s is the entropy density, and the factor β is assumed to be equal to $1/T$ in accordance with the well-known formula $dQ = Tds$. We ignore all the irreversible processes. For an ideal fluid, $q^i = 0$ and P_{ij} contains only the scalar P, as follows from (23) and (24). We now assume that the entropy density s depends on a finite set of extensive parameters, as in ordinary thermodynamics, and, in particular, that it is determined solely by the densities n and e, as for simple single-component systems. Calculating the rate of production of entropy by means of (23) and (24), we obtain

$$\dot{s} + su^r{}_{;r} = s_{,n}\dot{n} + s_{,e}\dot{e} + su^r{}_{;r} = [s - s_{,n}n - (e + P)\,s_{,e}]\,u^r{}_{;r}. \tag{33}$$

By the second law of thermodynamics, the left-hand side of (33) is a positive-semidefinite quantity, while the right-hand side is not, despite the circumstance that

$$P = -e + (s_{,e})^{-1}(s - s_{,n}n) = P\,(n,\ e), \tag{34}$$

which represents the first law of thermodynamics. The derivatives are defined as

$$s_{,n} = -\mu/T;\ s_{,e} = 1/T, \tag{35}$$

where μ is the chemical potential, T is the temperature,[27] and P is the thermodynamic pressure. Choosing a particular form of the function $s(n, e)$ by certain physical considerations, we can obtain from (34) the necessary relationship between P, n, and e.

Microscopic methods of deriving the equation of state

The equation of state describes the considered medium. In principle, it can be derived from the interaction between the particles by means of the methods of quantum statistics. In practice, only very simple "matter models" like that of an ideal gas can be solved in explicit form. Below, we list the basic methods of finding the equation of state.

I. *Bethe–Brueckner–Goldstone method.* This is based on partial summation of the two-particle collision amplitudes and introduces an effective interaction in the medium. The most recent results can be found in Ref. 28.

II. *Hartree–Fock method.* This is based on a Hamiltonian containing effective forces and introduces a self-consistent mean field. For zero-range forces, the equation of state is greatly simplified. The Skyrme interaction is often considered as an example. An equation of state at finite temperatures is derived, for example, in Ref. 29.

III. *Variational methods.* The total energy of the system is minimized by varying the three-particle function with the Jastrow ansatz. Various forms of this method have been developed, for example, cluster expansions. Partial summation leads to the hypernetted-chain method.[30]

Basically, all these methods are nonrelativistic; methods I and III take into account the particle correlations. Sometimes the equation of state violates the causality principle, i.e., the signal velocity may be superluminal.

IV. *Field-theoretical methods.* Starting from a Lagrangian of interacting fields, one can derive equations of motion from the components of the energy–momentum tensor[31] or by means of a partition function by applying a method of path integration.[32] In the majority of cases, it is sufficient to make a restriction to the mean-field approximation. Another method consists of finding the thermodynamic quantities in a discretized space–time (lattice) by direct computational methods. This approach is particularly popular in QCD.[12,33]

In our review we shall not devote much attention to the individual properties of different forms of matter. In the first place, we are interested in dynamical changes that occur in the matter during relativistic heavy-ion collisions. From this point of view, it is quite adequate to use phenomenological equations of state that reflect the experimentally observed properties of matter and that follow from estimates made in the framework of microscopic theories. Below, as an illustration, we give one of the possible forms of such an equation of state.

Matter confinement and deconfinement

Hydrodynamic calculations require much computer time, and it is therefore more convenient to use simple parametrized equations of state than ones which have been derived microscopically. In this section, we give the parametrization used in the present paper.

I. *Nuclear matter.* The specific energy W is usually divided into two parts; the first corresponds to cold compression, and the second to thermal compression:

$$W(n, s) = W_c(n) + W_{th}(n, \hat{s}) + m_n. \tag{36}$$

Here, W is a function of the baryon density n and the specific entropy $\hat{s}$. The temperature $T = (\partial W/\partial \hat{s})_n$ and the pressure $P = n^2(\partial W/\partial n)_{\hat{s}}$ can be obtained in explicit form from (36). The first term in (36) describes the compression energy of cold matter, which has a minimum at the saturation density of symmetric nuclear matter ($n_0 \simeq 0.16\ \mathrm{F}^{-3}$), and it is often approximated by a quadratic function. Since we are interested in reactions at high energies, where the temperature is above the Fermi energy, we use a high-temperature expansion for the thermal part in (36). The equation of state can now be written as

$$W = \frac{K}{18}(n/n_0 - 1)^2 + \frac{3}{2}T + \frac{\pi^2}{10}T^4/n + m_n; \tag{37}$$

$$\hat{s} = 2.5 - \lg\left\{\frac{n}{4}\left(\frac{2\pi}{m_n T}\right)^{3/2}\right\} + \frac{4\pi^2}{30}T^3/n, \tag{38}$$

where K is the coefficient of nuclear compressibility, extracted from relativistic heavy-ion collisions and monopole modes in heavy nuclei ($K \simeq 200$–300 MeV).[34] The second term takes into account the thermal excitations of the nucleons, while the third corresponds to thermal excitations of pions. For simplicity, we ignore both the rest mass of the pions and their interaction in the medium. We also ignore excitation of δ isobars (they would seriously violate the parametrization). Since we consider a relativistic medium, we take into account the nucleon rest mass, $m_n = 938$ MeV. Equation (38) for the entropy was obtained in the same approximation.

A different method of parametrization, proposed in Ref. 35, is based on more accurate division of W into potential and kinetic terms and appropriate allowance for the pions and δ isobars. This method also makes it possible to describe modern data on heavy-ion reactions, but it violates the causality principle in the density region in which we are interested. In contrast, our parametrization is free of this shortcoming.

II. *Quark–gluon plasma.* In the zeroth order of perturbation theory, the thermodynamic potential for the plasma has the form[3,5–7]

$$-\Omega(\mu_q, T) = P = \frac{37}{90}\pi^2 T^4 + \mu_q^2 T^2 + \mu_q^4/2\pi^2 - B. \tag{39}$$

The appearance of the bag constant B is a consequence of nonperturbative effects and reflects the difference between the QCD vacuum and the perturbative vacuum. We prefer to use the value $B = (235\ \mathrm{MeV})^4$, which has been obtained from hadron spectroscopy.[36] Equation (39) includes two quark flavors with degree of degeneracy $d_q = 12$ (with respect to spin, charge, and color) and gluons with degree of degeneracy $d_g = 16$ (with respect to helicity and color). Knowing the thermodynamic potential, we can readily find the energy density

$$e = \Omega - s\frac{\partial\Omega}{\partial T} - n\frac{\partial\Omega}{\partial\mu_q} = 3P + 4B \tag{40}$$

and the baryon density

$$n = -\frac{1}{3}\frac{\partial\Omega}{\partial\mu_q} = \frac{2}{3}\mu_q(T^2 + \mu_q^2/\pi^2). \tag{41}$$

Here, μ_q is the quark chemical potential; $\mu_q = \mu/3$, where μ is the baryon chemical potential. The terms of higher orders are discussed and calculated in Refs. 5 and 37.

Transport coefficients

General introduction

We now turn to the more general case when the effects of irreversibility are no longer vanishingly small but are still rather weak. We assume that all irreversibility is associated with transport processes; then the equilibrium state will be an isotropic spatial distribution, and any nonisotropy may lead to a disturbance of the equilibrium, this being an irreversible process. For moderate inhomogeneities, the principle of local equilibrium is valid,[27,38] i.e., in our case the local state is completely determined by the matter density n and the energy density e. We write

$$\left.\begin{aligned} q^i &= q^i_{(\mathrm{tr})}; \\ P^{ik} &= P(g^{ik} + u^i u^k) + P^{ik}_{(\mathrm{tr})}, \end{aligned}\right\} \tag{42}$$

where the index (tr) denotes the transport terms. Using now the conservation equations $T^{ij}_{;j}u_i = 0$ and $(nu^i)_{;i} = 0$, we can write down a positive-semidefinite entropy-production function $s^i_{;i}$ in the form

$$s^r_{;r} = (\beta - s_{,e})q^r_{(\mathrm{tr});r} + q^r_{(\mathrm{tr})}(\beta_{,r} + s_{,e}u_{r;i}s^i) - s_{,e}P^{rs}_{(\mathrm{tr})}u_{r;s} \geqslant 0. \tag{43}$$

The expected form of the transport equations is such that $q^i_{(\mathrm{tr})}$ and $P^{ik}_{(\mathrm{tr})}$ can be expressed in terms of local densities and their gradients. Since the term $q^j_{;j}$ in Eq. (43) cannot have a definite sign, the expression in the brackets must be zero:

$$\beta = s_{,e} = 1/T. \tag{44}$$

We arrive at the inequality

$$q^r_{(\mathrm{tr})}(T_{,r}+Ta_r)+TP^{rs}_{(\mathrm{tr})}u_{r;\,s}\leqslant 0. \qquad (45)$$

To get further, we impose on the system three simplifying conditions:

I. The temperature T is positive.

II. The matter is "simple" in the sense that the inequality (45) is separable in the two individual semidefinite terms that describe the different independent irreversibilities.[20]

III. The transport terms contain derivatives of the minimally necessary order and degree.

Conditions I and II are the ordinary conditions that lead to viscous and heat-conducting fluids; condition III is needed from the practical point of view, since even the classical case has been poorly studied outside the framework of a linear (Newtonian) fluid. Because of condition II, both terms in the sum (45) must be negative-semidefinite, and, restricting ourselves to terms linear in the first derivatives, we can obtain the general formulas

$$\left.\begin{aligned} &q^i_{(\mathrm{tr})}=-\varkappa(g^{ir}+u^iu^r)(T_{,r}+Ta_r);\\ &P^{ik}_{(\mathrm{tr})}=-\eta(u_{r;\,s}+u_{s;\,r})(g^{ir}+u^iu^r)(g^{ks}+u^ku^s)\\ &-\eta'(g^{ik}+u^iu^k)u^r{}_{;r}. \end{aligned}\right\} \qquad (46)$$

Here, the coefficients $\varkappa$, η, and η' are non-negative and by virtue of the principle of local equilibrium depend only on the extensive densities n and e.

The physical significance of these coefficients is readily seen from the relations (46), in which one can clearly trace the connection with classical heat conduction and viscosity. (Note, however, that the acceleration term q^i is neither a Lorentz term nor a gravitational effect, indicating that the general theory of relativity really is necessary here.) Then we can interpret $\varkappa$, η, and η' as the transport coefficients of the thermal conductivity and shear and bulk viscosity. [Instead of η', one sometimes introduces a different coefficient of bulk viscosity, $\zeta=\eta'-(2/3)\eta$, which includes the shear viscosity in such a way as to conserve the volume.] Relativistically, the thermal conductivity is expressed in terms of the gradient of μ/T, whereas in the nonrelativistic approximation it contains only the temperature gradient.

The equations $T^{ij}_{;j}u_i=0$ and $T^{ij}(g_{ik}+u_iu_k)=0$ together with (46) form the relativistic heat-conduction equation and Navier–Stokes equation. On the transition to a comoving coordinate system, one can show that the heat-conduction equation is an equation of parabolic type. Thus, we come up against the fact that the relativistic theory admits the propagation of superluminal signals. Some authors assert that well-chosen boundary conditions make it possible to avoid such signals.[39] Other authors[40] include in (46) additional gradients and introduce corresponding transport coefficients. As a result, one actually obtains hyperbolic equations like those derived microscopically from the Boltzmann equation by using Grad's moment method.[21]

Microscopic estimates of the transport coefficients

The structure of the dissipative terms in (46) is based on the Boltzmann equation. Expanding the nonequilibrium distribution about the equilibrium value f_0, we can express the deviation from equilibrium in terms of f_0, linearizing with respect to the gradients (using the Chapman–Enskog approach or Grad's moment method[21]). We then arrive at the structure of (46), and the phenomenological transport coefficients can be calculated microscopically. The calculations for an ideal Fermi gas contain a strong dependence on the density,[41]

$$\eta=\frac{\sqrt{m_n\pi(T+T_0)}}{8\sigma_{\mathrm{tot}}}, \qquad (47)$$

where σ_{tot} is the total nucleon–nucleon interaction cross section, and

$$T_0=9(3\pi^2n^2/2)^{2/3}/16m_n$$

is the effective temperature of a cold nucleon gas. The improved calculations made in Ref. 42 for nuclear matter lead to values that significantly exceed the simple estimate.[47] The bulk viscosity disappears in both the nonrelativistic and the ultrarelativistic cases. For example, the relation $\zeta=\eta'-(2/3)\eta=0$ holds for nuclear matter and for the plasma. Only in the intermediate region, in which the rest mass is comparable with the momentum of the particles, do we have $\zeta\neq 0$. The shear viscosity of the plasma can be estimated by means of the expression[43]

$$\eta=aT^3,\ a\sim 1,\ \ldots,\ 3. \qquad (48)$$

In the case of charge symmetry ($\mu=0$), there is no heat conduction in the medium.

3. DYNAMICAL PHASE TRANSITIONS

Model of a volume-averaged phase transition

In all dynamical processes, one observes a certain deviation from the equilibrium state, and this leads to a relaxation process.[38] Therefore, to describe such dynamical processes, phase transitions, or chemical reactions, it is necessary to use the methods of nonequilibrium thermodynamics. We consider the formation of a new phase. This is a particular example of the occurrence of a new component in the medium.

We suppose that the following condition is satisfied:

$$\left.\begin{aligned} &T^{ij}=xT^{ij}_{(1)}+(1-x)T^{ij}_{(2)};\\ &n^i=xn^i_{(1)}+(1-x)n^i_{(2)}, \end{aligned}\right\} \qquad (49)$$

where x is the fraction of the volume occupied by phase 1. Subsequently, we shall identify $T^{ij}_{(1,2)}$ with the energy–momentum tensor, which includes all bulk properties of phases 1 and 2, and, thus, we ignore surface contributions. We shall also assume that both phases belong to the common average velocity field. In this case, the energy–momentum tensor and the baryon current have the form of Eqs. (20) and (24)–(26), but the thermodynamic quantities are now averaged over the volume in accordance with

$$e=xe_1+(1-x)e_2;\ P=xP_1+(1-x)P_2\ \ldots \qquad (50)$$

The ordinary thermodynamic identities remain valid only for the individual components but not for the averaged components. It is expedient to introduce the specific weight of phase 1 as

$$x=xn_1/n. \qquad (51)$$

From the equation of motion (4) we can derive expressions for the change in the entropy:

$$\dot{\hat{s}} = \frac{2}{T_1+T_2}\left\{(\mu_2-\mu_1)\dot{\hat{x}} + (P_1-P_2)\dot{x}/n - \frac{1}{2}(T_1-T_2)\dot{\Delta}\right\},$$
$$\Delta \equiv \hat{x}\hat{s}_1 - (1-\hat{x})\hat{s}_2. \qquad (52)$$

The second law of thermodynamics, $\dot{\hat{s}} \geqslant 0$, presupposes a direction of the processes. In particular, there exist three types of relaxation processes, these being generated by differences of the chemical potentials, pressure, and temperature in the two phases. During the time of the relaxation process ($\dot{\hat{s}} = 0$)

$$\mu_1 = \mu_2;\ P_1 = P_2;\ T_1 = T_2. \qquad (53)$$

These conditions are known as the Gibbs condition for equilibrium of the two phases. In slow dynamical processes, one often uses the approximation of an equilibrium transition. Usually, the mechanical (pressure) and thermal (temperature) equilibria are reached more rapidly than the thermal equilibrium.[44] Therefore, the conditions $\mu_1 \neq \mu_2$, $P_1 = P_2$, $T_1 = T_2$ give a fairly good approximation for practical purposes. In a medium in which the flux is not conserved ($\mu = 0$), the analog of (52) can be written as

$$(su^i)_{;i} = \frac{2}{T_1+T_2}\left\{(P_1-P_2)\dot{x} + \frac{1}{2}(T_2-T_1)(\delta u^i)_{;i}\right\},$$
$$\delta \equiv xs_1 - (1-x)s_2. \qquad (54)$$

Since specific quantities do not occur here, there exist only two relaxation processes.

We shall call $\hat{x}$, x, and Δ evolution variables, denoting them below by ψ_α. To close the system of evolution equations (23) and (24), we also need relaxation equations for ψ_α. These may be either dynamical equations or additional restrictions on the evolution variables ψ_α. Below, we give three examples.

Dynamics of phase transitions

Given boundary conditions

If the thermodynamic variables satisfy additional boundary conditions, it is possible to determine the evolution in time of the variables ψ_α by integrating the equations of motion. A simple example is the case $T = \text{const}$ and $\mu_1 = \mu_2$, $P_1(\mu, T) \neq P_2(\mu, T)$. A special case is an equilibrium transition, $T = T_c$, where T_c is the critical temperature.

Linearized relaxation laws

In the spirit of linear phenomenological assumptions for the thermodynamic force–flux relations,[38] we can postulate the following relaxation equation for the evolution variables[46]:

$$\dot{\psi}_\alpha = -\frac{\psi_\alpha - \psi_{\text{eq},\alpha}}{\tau_\alpha}, \qquad (55)$$

where τ_α is the relaxation time. The deviation from equilibrium, $\psi_\alpha - \psi_{\text{eq},\alpha}$, leads to a change of the evolution variables. The equilibrium is approached in accordance with an exponential law in the time τ_α. The relaxation time τ_α must be determined microscopically, i.e., by calculating transition probabilities, nucleation rates, rates of growth, etc.

Droplet model

If one goes beyond the relaxation approximation, it is necessary to introduce a large number of input parameters. As an example, we consider the droplet model in the framework of the classical theory of nucleation. It is based on two concepts—nucleation and growth of a droplet. Let w be the probability of the appearance in unit space–time of a spherical droplet with critical radius R_c and growth rate v. Then

$$x(t) = \exp\{-h(t)\}, \qquad (56)$$

and the volume of the fraction is defined as

$$h(t) = \frac{4\pi}{3}\int_{t_c}^{t} w(\bar{t})\left[R_c(\bar{t}) + \int_{\bar{t}}^{t} v(\theta)\,d\theta\right]^3 d\bar{t}.$$

Equation (56) cannot be derived rigorously, but it has often proved to be a good approximation.[46] It is convenient to transform Eq. (56) into a differential equation of fourth order and solve it simultaneously with the other dynamical equations.

The classical expressions for the surface tension α of the droplet, its critical radius R_c, and the nucleation rate w have the form[47]

$$\left.\begin{aligned} &\alpha = \alpha_0 T_c^3; \\ &R_c = 2\alpha/|P_1 - P_2|; \\ &w = w_0 T_c^4 \exp\{-16\pi\alpha^3/3T\,(P_1-P_2)^2\}. \end{aligned}\right\} \qquad (57)$$

The exact determination of the slowly varying functions α_0 and w_0, which, as one expects, are quantities of order unity, is the subject of the discussions in Ref. 46. Details can be found, for example, in the literature on inflationary cosmology.[48]

Phase transitions are phenomena of collective nature. Therefore, one cannot assert in advance that the characteristic time scale of the model theory will be equal to the relaxation time τ_α. It must be emphasized that the relaxation time is determined by the dynamics. To demonstrate this, we consider an expanding and cooling system. The dynamical scale is $t_{\text{dyn}} \sim T/\dot{T}$, $n/\dot{n}$,..., whereas the nucleation time scale is

$$t_{\text{nuc}} \sim \{v^3 w\}^{-1/4}. \qquad (58)$$

[This expression follows from Eq. (56) after substitution of $R_c = 0$ and $T = \text{const}$.] Nucleation becomes important for times $t_{\text{dyn}} \sim t_{\text{nuc}}$ precisely in the case when the reheating associated with the release of latent heat compensates the primary cooling. Thus, from the condition $t_{\text{dyn}} = t_{\text{nuc}}$ one can find the supercooling and the corresponding order of the relaxation time. It was found that a critical ingredient is the surface tension, which in the case of deconfinement is estimated as $\alpha \sim (80\ \text{MeV})^3$ (Ref. 49).

4. IDEAL SHOCK WAVES

In compressible fluids, a perturbation propagates with the velocity of sound $v_s^2 = (\partial P/\partial e)_{\hat{s}}$. Shock waves are formed when special boundary conditions permit the appearance of supersonic velocities in the medium. The shock front divides the fluid into two regions in different states. In the limit of vanishing dissipative effects, i.e., for an ideal fluid, the width of the front tends to zero. As the shock front passes through the fluid, the change in the state is determined by the conservation laws for the number of particles, energy, and momentum. The relation connecting the state in front of the shock wave and behind it is known as the Rankine–Hugoniot (RH) adiabat. It generalizes the ordinary Poisson adiabat for abrupt changes leading to entropy generation.

Several theoretical studies (Refs. 4–7 and 50–55) have been made of the formation of shock waves in heavy-ion collisions. The Rankine–Hugoniot relation makes it possible to obtain a fairly complete picture of the hydrodynamic problems without recourse to solution of the hydrodynamic equations. In recent years, such investigations have been made in connection with a cosmological phase transition,[50] the growth of bubbles in a supercooled plasma with vanishingly small baryon density,[51] hadronization of an expanding plasma with finite[56] or zero[57] baryon density, and the formation of a plasma with a high baryon density.[3,55] The methods of treating nuclear phenomena find application in technical physics for the description of the change of materials under the influence of a shock wave.[58]
of treating nuclear phenomena find application in technical physics for the description of the change of materials under the influence of a shock wave.[58]

Derivation of the equation of the shock adiabat

We consider a plane shock front propagating in a fluid with velocity $w^i = (\gamma, \gamma\mathbf{w})$. The regions to the two sides of the front are the initial (0) and final (1) states. These states are described by two thermodynamic variables (n and T) and two velocities (u_0 and u_1) in front of the shock wave and behind it, respectively. It is convenient to introduce the vector Λ^i normal to the direction of propagation of the shock front and possessing the property

$$\Lambda^i \bar{w}_i = 0;$$
$$\Lambda^2 = \Lambda^i \Lambda_i = \begin{cases} +1 \text{ for spacelike vector,} \\ -1 \text{ for timelike vector.} \end{cases} \quad (59)$$

Usually, the velocity w_i of the shock wave is a timelike vector, and then $\Lambda^i = (\overline{w}, \overline{\mathbf{w}}/\overline{w})/\sqrt{1-\overline{w}^2}$ must be a spacelike vector. However, in the general case $\overline{w}^i$ may well be spacelike if one is considering a transition that takes place in the complete volume of the fluid. By means of the normal vector Λ_i we can define the flux of particles that cross the shock front as

$$j_0 = n_0 u_0^i \Lambda_i; \quad j_1 = n_1 u_1^i \Lambda_i. \quad (60)$$

Integrating the equations of motion (18) and (19) along the direction perpendicular to the front, we find

$$[j] = [n u^i \Lambda_i] = 0; \quad (61)$$
$$[R^i] = [T^{ij} \Lambda_j] = 0, \quad (62)$$

where the symbol [ ] denotes the "jump" $Q_1 - Q_0$ of the quantities across the shock front. At this stage, one introduces the generalized specific volume $x = (e+P)/n^2$, which plays the same role as the specific volume m_n/n in the nonrelativistic case. Then the vector equation (62) is split into two parts by means of the projection operators Λ^i and $\mathscr{P}^{ij} = g^{ij} - \Lambda^i \Lambda^j / \Lambda^2$, which are continuous on crossing the shock front. From Eq. (60) and $[R^i \Lambda_i] = 0$ we find

$$j^2 = -\Lambda^2 \frac{[P]}{[x]}, \quad (63)$$

whereas from $[R^i \mathscr{P}_{ik} R^j \mathscr{P}^k_j] = 0$ we obtain

$$j^2 = \Lambda^2 [(e+P)x]/[x^2]. \quad (64)$$

Equating the last two expressions, we can eliminate all the kinematic variables and arrive at the Rankine–Hugoniot–Taub (RHT) adiabat[60]:

$$P_2 - P_1 = (x_1 n_1^2 - x_0 n_0^2)/(x_0 + x_1). \quad (65)$$

Equation (65) is the relativistic generalization of the Rankine–Hugoniot relation. It has the same form for normal ($\Lambda^2 = 1$) and timelike ($\Lambda^2 = -1$) shock waves. The velocities of the fluid in front of and behind the shock wave in the system in which the shock front is at rest can be calculated from Eqs. (60), (63), and (65) by means of the vectors $\Lambda = (0, 1)$ and $\Lambda^i = (1, 0)$, respectively, as

$$v_0^2 = \left[\Lambda^2 \frac{(P_1 - P_0)(e_1 + P_0)}{(e_1 - e_0)(e_0 + P_1)} \right]^{\Lambda^2}. \quad (66)$$

The expression for v_1 can be readily obtained from (66) by interchanging the indices 0 and 1.

For $\Lambda^2 = -1$, a velocity relative to the timelike front has no meaning, and therefore one can choose $v_0 = 0$ and, thus, obtain

$$v_1 = 0; \ [n] = 0; \ [e] = 0. \quad (67)$$

Since the two states are separated in time, the case $\Lambda^2 = -1$ signifies an instantaneous transition in the complete volume. It follows from Eq. (63) that such a transition is impossible if the Rayleigh line connecting the states 0 and 1 has a positive slope.

In the general case, when the state of the matter changes its phase structure, it is necessary to distinguish two types of wave[15,51,59]—detonation waves with $v_1 < v_0$ and deflagration waves with $v_1 > v_0$. Considering these processes in the self-frame of the fluid in the initial state, one can see that a detonation front advances inwards, whereas a deflagration front is directed outwards with respect to the initial state.

Properties of the Rankine–Hugoniot–Taub adiabat

Figure 1 shows the RHT adiabat $p(x)$ for the transition from the initial state 0 to a set of states 1. Since in this case the phase of state 1 differs from the initial phase, the point 0 does not lie on the curve. The slope of the Rayleigh line between the points 0 and 1 determines the particle flux in accordance with Eq. (63). The change of this flux is associated with the change of the specific entropy:

$$\frac{dj_1^2}{ds_1} = \frac{2x_1 n_1 T_1}{(x_1 - x_0)^2} > 0. \quad (68)$$

This relation is obtained after differentiation of Eq. (65) and the introduction of the specific entropy in accordance with

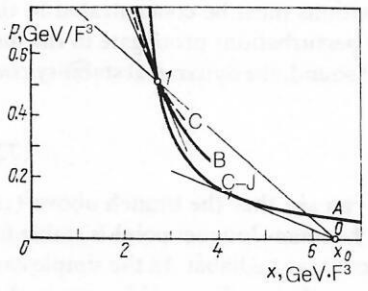

FIG. 1. Shock adiabat A for a complete phase transition from the initial state 0 with Chapman–Jouguet point (C–J). Curves B and C are the shock and Poisson adiabats that pass through the final point 1.

the first law of thermodynamics: $de = nTd\hat{s} + \{(e+P)/n\}dn$. The adiabat of phase 1 is drawn through point 1 in Fig. 1. The two curves have a point of tangency of the third order, but they are not parallel to the RHT adiabat. The velocity associated with the slope of the Poisson adiabat depends on the velocity of sound as $(u_{1s}n_1)$, whereas the slope of the straight line 0–1 is less, from which it follows that $u_1 < u_{1s}$.

On the RHT adiabat there may exist a singular point, at which the tangent passes through the initial point 0. Such a point is known as a Chapman–Jouguet (C–J) point. At this point, the variation of dj, $-a$ by virtue of (68), and therefore $d\hat{s}$ vanishes as well. Then the velocity of the fluid behind the shock front is equal to the velocity of sound:

$$v_1^2 = \frac{u_1^2}{1+u_1^2} = \frac{-(\partial P/\partial x)_{\hat{s}}}{n_1^2-(\partial P/\partial x)_{\hat{s}}} = \left(\frac{\partial P}{\partial e}\right)_{\hat{s}}. \tag{69}$$

At the Chapman–Jouguet point, the flux and the entropy reach extrema. Using Eqs. (63) and (69), we can calculate the change in the velocity of the matter behind the shock wave compared with the change of the velocity of sound in this fluid:

$$\frac{d}{dP}\left(\frac{u_1^2}{u_{1s}^2}\right)_{C\text{-}J} = \frac{d}{dP}\left(-j^2\frac{dx}{dP}\right)_{C\text{-}J} = -j\left(\frac{d^2x}{dP^2}\right)_{C\text{-}J}. \tag{70}$$

Thus, above the Chapman–Jouguet point the velocity becomes greater than the velocity of sound for a convex shock adiabat, $d^2P/dx^2 > 0$, and less than the velocity of sound for a concave adiabat, $d^2P/dx^2 < 0$. The existence of such a point depends on the thermodynamic properties of the matter. In the nonrelativistic case, such a point occurs only on a concave adiabat and only for a thermodynamically anomalous medium with $d^2(1/n)/dP^2 < 0$.

Instability

A necessary condition for the existence of a shock wave is a growth of entropy when the shock wave passes:

$$[su^i\Lambda_i] \geqslant 0. \tag{71}$$

However, this condition is not sufficient, and it is therefore necessary to consider as well some dynamical aspects. A detailed analysis of the conditions for stability in the nonrelativistic case can be found in Ref. 62. Another necessary condition for stability of a shock front, which prevents the front from becoming smoother or breaking up, is that the perturbations of the thermodynamic quantities in the final state must propagate more rapidly than the front itself. In the initial state, the perturbations must be concentrated in the shock front. Since weak perturbations propagate in the medium with the velocity of sound, the dynamical stability conditions take the form

$$u_0 > u_{0s};\ u_1 < u_{1s}. \tag{72}$$

Considering Fig. 1, we can see that the branch above (respectively, below) the Chapman–Jouguet point is stable for a convex (respectively, concave) adiabat. In the simple case without a phase transition, the condition (72) means that for a normal medium ($d^2P/dx^2 > 0$) in the process of contraction a stable shock front appears, whereas for a rarefaction process there is no shock front.

As an illustration of these conditions,[61] we consider the RHT adiabat (65) for transition from normal nuclear matter with $x_0 = W_0/n_0^2 \approx 6.3$ GeV·F^3 and pressure $p_0 = 0$ to a noninteracting quark–gluon plasma with equation of state (41). Then the adiabats for the different values of the bag constant B are determined as

$$P_1 = \frac{x_0W_0 - 4Bx_1}{3x_1 - x_0}. \tag{73}$$

These adiabats, which are shown in Fig. 2, are hyperbolas centered around $(x_1p) = (x_0/3,\ -4B/3)$. For $B^{1/4} = (W_0/4)^{1/4} \simeq 130$ MeV, the RHT adiabat passes through the initial point. For smaller values of B, the adiabat has a Chapman–Jouguet point, above which the matter velocity behind the shock front is less than the velocity of sound, as a result of which the shock wave is stable. For $B^{1/4} = (3W_0/4)^{1/4} \simeq 171$ MeV, the RHT adiabats have the property $dP/dx > 0$, a property that is unknown for nonrelativistic problems. These curves have a further singular feature, namely, in the region to the left of curve (b) in Fig. 2 we have $dn/dj < 0$. However, this behavior does not lead to a decrease of the entropy, in contrast to the nonrelativistic case,[15] for which the inequality $dn/dj > 0$ is equivalent to the condition of increase of the entropy. In Fig. 2, curve (a) corresponds to the condition of dynamical stability [see Eq. (72)], in accordance with which all the adiabats with positive slope and the adiabats situated above the Chapman–Jouguet point correspond to stable shock waves. The condition (71) on the entropy is equivalent to the requirement $T > 0$, and is represented in Fig. 1 by curve (b). The RHT adiabat for a phase transition of the first kind is more complicated and is considered in Sec. 5.

Width of the shock front

Hitherto, we have ignored the finite width of the shock front. From the microscopic point of view, the front must have a width not less than the particle mean free path, this ensuring the formation of the new state as a result of the particle collision. In the hydrodynamic picture, this mechanism of generation is simulated by the dissipative terms. These terms also lead to an increase of the entropy in a shock wave of finite thickness. For simplicity, we discuss the effect of viscosity in the one-dimensional case, for which the shear viscosity plays the same role as the bulk viscosity, and we consider them together, introducing an effective viscosity:

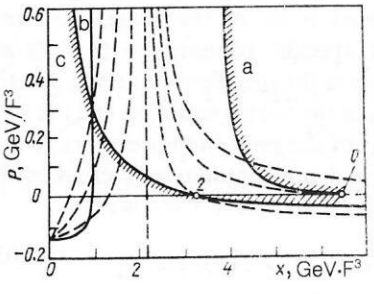

FIG. 2. Regions (hatched) of occurrence of a stable shock wave as determined by conditions on the dynamics (curve a), entropy (curve c), and the pressure, $P < 0$ (curve d). Curve b corresponds to the condition $dn/dj = 0$.

$$T^{ij} = (e + P)\, u^i u^j + (P + \eta_{ef} u^k{}_{,k})\, g^{ij},$$
$$\eta_{ef} = 2\eta' + \eta. \tag{74}$$

The second equation holds exactly only in the nonrelativistic case. From the energy–momentum tensor (74), by analogy with Eqs. (25)–(27) and in accordance with the first law of thermodynamics, $\dot{e} = nT\dot{\hat{s}} + (e+P)\dot{n}/n$, we obtain the following expression for the change in the entropy:

$$\dot{s} = \frac{\eta_{ef}}{nT}\left(\frac{\dot{n}}{n}\right)^2. \tag{75}$$

We apply (75) to the case of a shock front of width Δl. Since the RHT relation determines the change of the entropy, we can, using the conservation laws, estimate Δl, which is necessary to find the dissipative forces. Making the approximation $\dot{s} \sim \Delta\hat{s}/\Delta l \overline{W}$, we obtain for the width of the shock front a value proportional to the coefficient of viscosity:

$$\Delta l = \eta_{ef} \frac{(n_1 - n_0)^2 \overline{W}}{\left(\frac{n_1+n_0}{2}\right)^3 \left(\frac{T_1+T_0}{2}\right)(\hat{s}_1 - \hat{s}_0)}. \tag{76}$$

An estimate of the viscosity force can be obtained from Eqs. (47) and (48). Using the value $\eta_{ef} \simeq 100\ \text{MeV/F}^2$, we obtain $\Delta l \sim 1$ F for transition to strongly compressed quark matter in the case of a bombarding energy of 7 GeV/nucleon. This width of the front is appreciably less than the nuclear diameter. At lower energies, the width increases somewhat.

Another reason for the appearance of a finite width of the shock front is the finite time τ of the phase transition. It is expected that the contribution is of order $\Delta l \sim (v_0 + v_1)\tau/2$. This effect is important for slow phase transitions with $\tau > 1$ F/sec.

Profile of the shock front

We can get a deeper picture of the behavior of the thermodynamic quantities on the shock front by solving the hydrodynamic equations in a system moving with the front. In this stationary case, Eqs. (18) and (19) simplify:

$$(nu^x) = (nu^x)_0;\quad T^{0x} = (T^{0x})_0;\quad T^{xx} = (T^{xx})_0. \tag{77}$$

The asymptotic quantities on the right-hand side of (77) must be calculated by means of Eq. (65). Using the energy–momentum tensor (74), we can find two coupled equations for the velocity and chemical potential[42]:

$$\left.\begin{aligned} \frac{du}{dx} &= \frac{P(1+u^2) - eu^2 - (T^{xx})_0 (1+2u^2) + 2(T^{0x})_0 \sqrt{1+u^2}\, u}{\eta_{ef}(1+u^2)}; \\ \frac{d(\mu/T)}{dx} &= \frac{(e+P)\, n\left[-eu + (T^{0x})_0 \sqrt{1+u^2} - (T^{xx})_0 u\right]}{T^2 \varkappa u^2}. \end{aligned}\right\} \tag{78}$$

In the case of vanishingly small coefficients of viscosity η_{ef} or thermal conductivity $\varkappa$ the numerator of the first or second equation, respectively, must also tend to zero. Equation (78) must be solved for initial conditions corresponding to small perturbations directed toward the final state determined by the RHT relation.

5. FORMATION OF PLASMA. ONE-DIMENSIONAL TREATMENT

Phase diagram and stopping power of nuclear matter

We now discuss the excitation and decay of a quark–gluon plasma in relativistic heavy-ion collisions. The nature of the deconfinement phase transition is still far from a complete understanding. This is due to the complexity of the problem of describing matter that consists of strongly interacting particles. The most reliable results are based on QCD calculations on a lattice. In the framework of purely gauge SU(3) theories it has been shown that there exists a phase transition of the first kind, characterized by a transition temperature of about 200 MeV and latent heat 1–2 GeV/F^3.[86] When light quarks are included in the treatment, the phase transition may become one of the second kind or even be altogether absent, though this is accompanied by dramatic changes of the energy density.[86] For a plasma with finite baryon density, the estimates of Ilgenfritz and Kripfganz[72] indicate the possibility of a phase transition of the first kind. Besides these lattice results, phenomenological approaches are also often used to describe the phase transition.[49,63]

Bearing in mind this complicated situation, we construct the phase diagram on the basis of the equations of state for nuclear matter (37) and (38) and for the quark–gluon plasma (39). Using the Gibbs criteria (53), we obtain the phase diagram shown in Fig. 3. The parameters of Eqs. (37)–(39) are fixed by choosing the values $K = 0.3m_n$, $n_0 = 0.16\ \text{F}^{-3}$, and $B^{1/4} = 235$ MeV. The hatching in Fig. 3 indicates the boundary region in which the two phases exist together. This region is fairly broad in the density interval between $5n_0$ and $12n_0$ for zero temperature and is bounded above by a temperature of about 170 MeV.

All our investigations which follow are based on this phase diagram. A distinctive feature is the fact that the significant difference between the degrees of freedom in the confinement and deconfinement states leads to a large difference between the entropies of these two states and to a large latent heat, of order $4B \simeq 1.5\ \text{GeV}\cdot\text{F}^{-3}$. This energy is needed to "melt" the hadrons into the plasma of the quarks and gluons. This general picture is in agreement with the lattice calculations. In this section, we investigate the processes of formation of the quark–gluon plasma in connection with the following questions.

What amount of energy is needed to attain the plasma state? How rapidly must the phase transition occur? What are the consequences of the finite time of the phase transition?

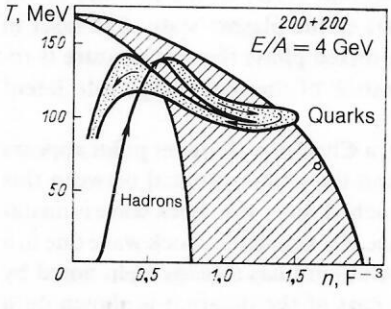

FIG. 3. Phase diagram of the matter. The hatched strip is the region of coexistence of normal nuclear matter and the quark–gluon plasma. The dotted area corresponds to different trajectories in the phase plane in a heavy-ion collision with energy $E/A = 4$ GeV, calculated in the one-dimensional model. The small open circle gives the predictions of the shock-wave model.

We give the treatment in a one-dimensional model, ignoring the transverse expansion of the system; as a result, the estimate of the energy needed to attain the plasma state may be somewhat too high. Comparison with two- and three-dimensional calculations[64] shows that the overestimation for the temperature and density is about 20%. Another source of error is the transparency effect, which is completely ignored in single-fluid hydrodynamics. In our model we assume instantaneous deceleration and local thermalization. If the nuclei come to rest in the interaction, this approximation may be justified. Earlier estimates[65] predict for the upper limit of complete stopping an energy of order 10 GeV/nucleon in the laboratory system. The recent information on the degree of deceleration of incident protons in nuclear matter[66] contains the optimistic prediction that heavy nuclei like those of uranium may be stopped in a central collision at energies right up to 30 GeV/nucleon.[67] In Sec. 6, we consider this aspect in the framework of a two-fluid model. At the same time we restrict ourselves to reactions with initial energies up to $E/A = 7$–10 GeV, remembering that these results will be only approximate in a discussion of processes that occur in relativistic heavy-ion collisions.

Shock-wave model

An idea of the problems that arise in the study of phase-transition dynamics can already be obtained at the level of the RHT relations. In a subsequent stage, we shall make the treatment more precise, investigating a linear solution of the hydrodynamic equations. For attainment of the plasma state, penetration into the region of phase coexistence is necessary (see Fig. 1). In this region, the matter is a mixture of nuclear matter and quark–gluon matter. A suitable variable for describing the fractions of the matter in the two phases is the evolution variable x introduced earlier by Eqs. (49) and (51). In the case of thermodynamic equilibrium, the evolution variable is a single-valued function of the density and temperature,

$$\hat{x}_{\text{eq}} = \frac{n_0(T)\,(n - n_1(T))}{n\,(n_0(T) - n_1(T))}, \qquad (79)$$

whereas in the region of pure phases $\hat{x}$ takes the values 1 and 0. The quantities $n_0(T)$ and $n_1(T)$ in Eq. (79) determine the lower and upper limits of the baryon density in the phase-coexistence region calculated in accordance with the Gibbs criteria (53). Figure 4 shows the RHT adiabat.[61] The curve consists of three parts, the first of which (OA) corresponds to nuclear matter, the second (AB) to the mixture of the phases, and the final part to the plasma state. The inset in Fig. 4 shows that in the mixed phase the temperature is reduced by the transformation of thermal energy into latent heat of the plasma.

In the mixed phase, a Chapman–Jouguet point appears on a concave adiabat, and the points situated between this point and B cannot be reached, since the shock wave is unstable. The possible existence of an unstable shock wave due to a phase transition of the first kind has already been noted by Bethe.[68] In Fig. 5, this part of the diagram is shown on a larger scale. Let us now consider whether breakup of the shock wave is possible when the first wave leads to the Chapman–Jouguet point and the second wave to the final state. Such investigations were also made in Refs. 56, 62, and 63. We calculate the shock adiabat that emanates from the

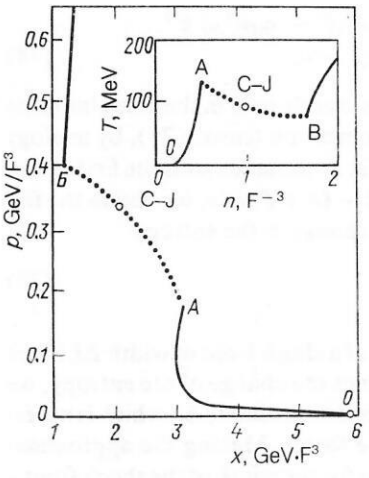

FIG. 4. The RHT adiabat for the two-phase model with Chapman–Jouguet point in the region of coexistence. The dependence of the temperature on the density is shown in the inset for the same system.

Chapman–Jouguet point (broken curve in Fig. 5). It can be shown that the initial velocity v_0 in the second shock wave is always less than the velocity of sound. Therefore, the condition (72) is violated, and the second shock wave is unstable. Above the Chapman–Jouguet point, where the initial velocity reaches the velocity of sound, only an isolated shock wave is stable, whereas the second wave propagates faster than the first. Thus, in the interval of energies $E/A \simeq 3.1$–4.3 GeV, to which the points of the interval (C–J, B) correspond, an unstable double shock wave is expected. The distance between the front increases as the difference of the velocities, multiplied by the time.

One can establish whether such an unstable shock wave occurs in small systems such as nuclei from a dynamical calculation, and the result depends on the amplitude of the dissipative forces and on the particular initial conditions.[69] In this connection, it should be recalled that the part of the RHT adiabat that is stable in the region of the mixture of

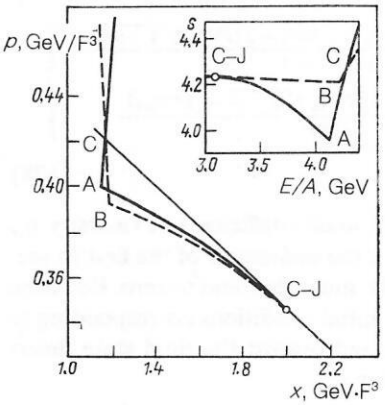

FIG. 5. The RHT adiabat (continuous curve) that begins at cold nuclear matter and the adiabat that emanates from the Chapman–Jouguet point (broken line). The tangent to the adiabat at the point C–J (thin line) determines the maximal (C–J) and minimal (C) energy below and above which shock waves are stable. The inset shows the entropy for both mechanisms as a function of the projectile energy.

phases leads to a broadening of the shock front, since usually the phase transition takes place more slowly than simple compression.

Increase of both the bag constant B and, in the first place, the compressibility parameter K leads to a shift in the position of the Chapman–Jouguet point in the direction of the region of nuclear matter. If this point reaches the boundary A, beyond which phase mixing occurs, a double shock wave may arise, as can be seen from Fig. 6. The two shock adiabats are represented in the figure by the lines OA and AB. A necessary condition for stability of the second shock wave is that the slope of the adiabat above the Chapman–Jouguet point be less than the slope of the Rayleigh line C–J–B and that both be less than the slope of the line O–C–J.

These ideas about the shock waves were verified by numerical solution of the hydrodynamic equations (18) and (19) with allowance for viscosity effects determined by Eq. (47). The results for initial collision energies $E/A = 2.5$ and 5 GeV are given in Fig. 7. These energies are situated below and above the instability region shown in Fig. 5, and lead to the appearance of fairly sharp shock fronts For energies $E/A = 3.5$ and 4.2 GeV, this sharpness of the fronts is lost, and their widths increase with increasing reaction time (Fig. 8). Despite this, the resulting final state is in good agreement with the prediction of the shock-wave model. The phenomenon of a double shock wave predicted in Fig. 6 is also confirmed in the numerical calculations (Fig. 9).

The detailed behavior of the density and temperature in a stable shock front can be best investigated by solving Eq. (78) for steady profiles. Figure 10 shows the density profiles of shock waves for initial energy $E/A = 7$ GeV. The nonmonotonic behavior of the temperature is a consequence of the release of the latent heat of melting at the phase transition of the first kind, which takes place precisely at the shock front.

Summarizing these investigations, we can say that the simple picture of a stable shock wave is fully adequate for reactions with relativistic heavy ions if the phase transition takes place sufficiently rapidly. This is possible because the stability of the shock wave persists in a wide range of initial energies. Instabilities can arise in certain intervals of the RHT adiabat in the transition region from the state of a mixture of phases to the plasma state. The width of the shock front obtained with allowance for the viscosity in accordance with (47) is small compared with the dimensions of

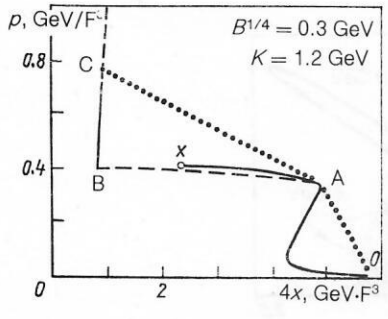

FIG. 6. Shock adiabat that begins at cold nuclear matter and ends at the point X in accordance with the condition $T \geqslant 0$ for some unrealistic values of the parameters given in the figure. For $E/A = 8.5$ GeV, a stable double shock wave OAB occurs.

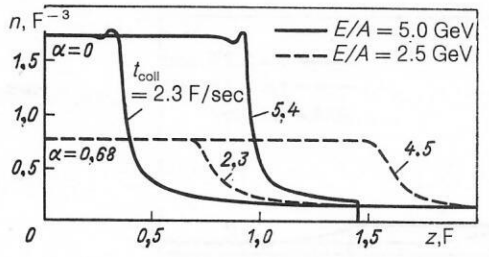

FIG. 7. Density profiles for a collision of two layers simulating the interaction of uranium nuclei as a function of the distance from the center of the collision at different times t_{coll}. The quantity α determines the relative amount of nuclear matter in the region behind the shock front.

the system. Even for large values of the coefficients of viscosity obtained in recent estimates,[43] the mean width of the shock front remains of order 1 F. In accordance with Eq. (76), the width of the front decreases with increasing initial energy. However, the effect of the quark and gluon degrees of freedom may lead to a significant increase of the viscosity.[43]

Delayed phase transition

Hitherto, we have assumed that the phase transition takes place fairly rapidly and that the state of thermodynamic equilibrium is always attained. We now consider the case when the transition time becomes comparable with the time of the complete collision process. All hadron–hadron collisions contribute to the thermodynamic ($T_1 = T_2$) and mechanical ($P_1 = P_2$) equilibrium, whereas the chemical equilibrium ($\mu_1 = \mu_2$) is realized by hadron reactions, which can be hindered by potential-barrier effects.[13] Therefore, in (53) we omit the condition $\mu_1 = \mu_2$ and will describe the state of the matter by the three variables n, T, and $\hat{x}$.

To solve the problem, we need one further equation for the variable $\hat{x}$, which characterizes the composition of the matter; in accordance with (55), we take this to be the linearized relaxation equation

$$\dot{\hat{x}} = -(\hat{x} - \hat{x}_{eq})/\tau, \qquad (80)$$

where $\hat{x}_{eq}$ is determined by Eq. (79). The relaxation time τ is usually taken to be equal to the characteristic QCD scale, $\hbar/B^{1/4} \sim 1$ F/sec. As yet there have been only a few attempts to give more realistic estimates of the relaxation time; these are in the interval from $\tau = 0.1$ (Ref. 70) to 1 F/sec.[13] It is possible that the inverse transition from the plasma state to the state of hadronic matter may be hindered, since it is necessary to form a color singlet from quarks distributed ran-

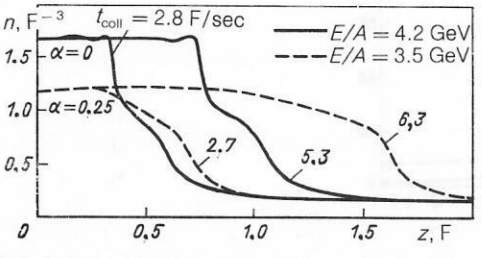

FIG. 8. The same as in Fig. 7 but for collisions in the region of formation of an unstable shock wave (see Fig. 7 for an explanation of the notation).

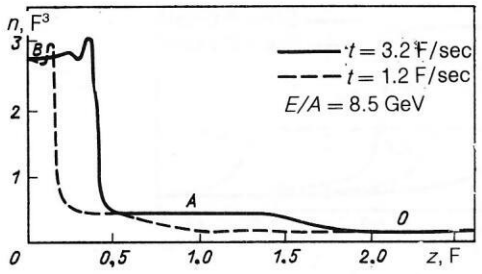

FIG. 9. Density profiles for the stable double shock wave predicted in Fig. 6.

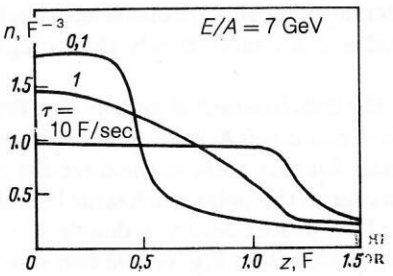

FIG. 11. Density profiles calculated for different relaxation times τ. For $\tau < 0.1$ F/sec, the central density is lower than the value predicted by shock-wave theory.

domly with respect to the color quantum number. Therefore, we shall use different values of τ in the compression ($\dot{\hat{x}} < 0$) and expansion ($\dot{\hat{x}} > 0$) stages.

In the case of a delayed phase transition, the validity of the shock-wave model is not obvious, since the expected width of the shock front is $\Delta l \sim \tau \sim 1$ F. For this reason, Eqs. (18) and (19) are solved numerically. The one-dimensional relativistic calculations were made by a method that was first used in nuclear physics. This method is based on the use of a synchronous, comoving curvilinear coordinate system and has hitherto been used only in astrophysical problems.[71] We modified it for the case of plane-wave geometry. The heavy-ion collision is modeled by the collision of flat layers of thickness 11 F, corresponding to a collision of two uranium atoms.

The influence of the finite transition time τ on the width of the shock front for initial energy $E/A = 7$ GeV is shown in Fig. 11. The estimate given in Sec. 4 is in good agreement with this numerical result. We shall show below that a relaxation time of order 1 F/sec already leads to a significant smearing of the shock front and an appreciable decrease of the final density in comparison with a fast transition. Even longer relaxation times completely wash out the shock-wave picture and lead to a moderate compression of the matter, for which it is no longer possible to achieve a complete phase transition. The effect of a very slow phase transition can also be described by increasing the effective viscosity.[43]

For the central fluid element, Fig. 12 shows typical trajectories in the temperature–density plane. In the hadronic phase, the temperature initially increases rapidly, but then, as soon as the boundary of the phase region has been reached, begins to fall because of the loss on latent heat. In the quark–gluon matter, the temperature again increases until the turning point is reached. For energy below $E/A = 4$ GeV, the turning point is in the region of phase coexistence, and its position is very sensitive to a change in the energy and the relaxation time. This can be seen in Fig. 13, in which the conditions of stability are not satisfied and all fluid elements describe different trajectories.

A remarkable property of these calculations at an energy below 10 GeV/nucleon is the fact that the temperature never exceeds the value 160 MeV, although our model overestimates the temperature. The same upper limit on the temperature has been found by other authors (Refs. 3, 55, 72, and 73). For energies $E/A \geqslant 4$ GeV, a stable shock wave appears under the condition $\tau < 1$ F/sec. Otherwise, one observes a weaker shock wave, which compresses the matter in the state of a mixture and which is followed by a region in which the matter is slowly transformed into the plasma. As an illustration, Fig. 13 shows the evolution of $\hat{x}$, which is fairly sensitive to the relaxation time τ. In the expansion stage, the quark matter is cooled until the phase boundary is crossed, after which the hadronization process commences and the latent heat is released. Irrespective of the initial energy, the matter reaches a very low density and high temperature (about 155 MeV), which is somewhat below the critical point of the phase transition.

As a result, we find that with increasing initial energy the formation of the plasma takes place rather smoothly. Even at energy $E/A \simeq 2$ GeV a certain percentage of the matter undergoes transformation. This fraction increases with increasing energy of the bombarding nuclei, though it is also sensitive to the transition time. This circumstance makes it

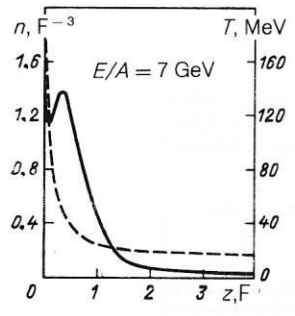

FIG. 10. Profiles of the density and temperature (broken curve) at the shock front. The values of the shear viscosity η_D were calculated in accordance with Ref. 42.

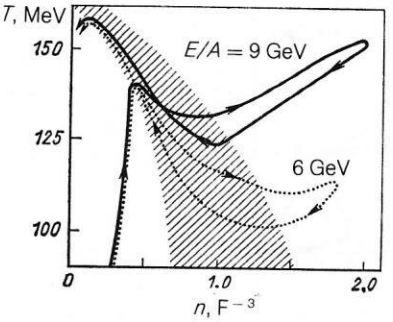

FIG. 12. Typical trajectories in the n–T phase plane for heavy-ion collisions at two values of the collision energy. The hatching identifies the region of phase coexistence.

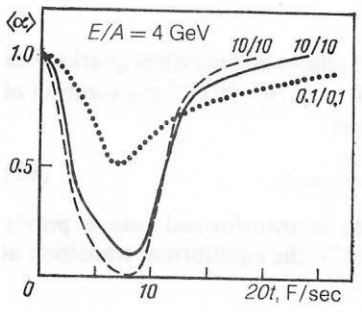

FIG. 13. Evolution in time of the composition of the nuclear matter for different values of $g = 1/\tau$, the rate of transformation from the stage of compression and expansion of the matter.

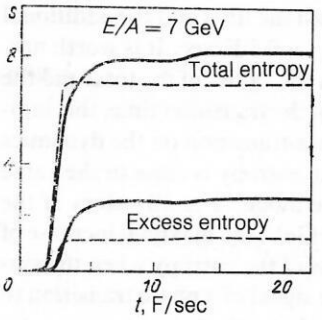

FIG. 14. Entropy per baryon as a function of the collision time in the center-of-mass system for relaxation time $\tau = 0.1$ F/sec (broken curve) and 1 F/sec (continuous curve). The lower part shows the excess entropy calculated in accordance with Eq. (81).

difficult to observe a definite threshold behavior when the phase transition occurs, since the appearance of the plasma is a gradual process.

Growth of the entropy

During the time of the collision, the heavy ions, which were initially cold, are heated, and the kinetic energy of their relative motion is redistributed in a random manner between many degrees of freedom. In a microscopic approach, the process can be modeled by means of the relativistic Boltzmann equation. In Ref. 74, this equation was solved for a spatially uniform distribution of particles. It was found that there is a rapid growth of the entropy, which reached saturation during a time 3–5 F/sec at energy $E/A \simeq 2$ GeV. The value of the entropy was found to be very close to the value obtained by solving the RHT equation. More detailed calculations made in the framework of the intranuclear-cascade model[75,76] also lead to values of the entropy close to the predictions of the RHT theory. Similar results have been obtained in hydrodynamic calculations.

The determination of values of the entropy from experiments is based primarily on analysis of the relative yields of the light fragments. Siemens and Kapusta[78] were the first to relate the entropy to the measured deuteron–proton ratio. The high values of the entropy obtained in this way were a long-standing puzzle for physicists. It has now become clear that many different mechanisms influence the production of light fragments: the finite size of the clusters[79] and the source,[80] suppression by virtue of the Pauli principle (nuclear Mott effect)[81] and decay of unstable light fragments,[77] and the appearance of a phase transition of the liquid–gas type.[82]

In hydrodynamics without allowance for viscosity, the entropy cannot increase as long as we are dealing with continuous solutions. The only possibility is provided by the shock-wave mechanism considered in Sec. 4. Then the change in the entropy can be estimated in terms of the RHT relation. In numerical calculations based on the use of a finite grid, the integral form of the hydrodynamic equations is used in implicit form and also leads to an increase of the entropy. In hydrodynamics with viscosity, a growth of the entropy is ensured by the action of the viscosity terms. It follows from the results of our calculations that the increase of the entropy in the shock wave does not depend on the value of the viscosity as long as the width of the shock front is small. This fact was used in (76) in the derivation of the expression for the width of the shock front. Such a treatment cannot be used in the expansion stage of the system, when the shock wave is unstable. Here, an increase of the entropy arises because of the influence of the viscosity. Estimates showed that in this stage there may be an additional growth of the entropy by 10–20%.[85]

A source of additional entropy is a delayed phase transition. If the collision process is slow, then the Gibbs conditions are satisfied and the phase transition is reversible. However, for a rapid change the Gibbs conditions are violated and the entropy increases in accordance with Eq. (52). In the model used in the previous subsection, the amount of additional entropy can be calculated as

$$\dot{s}_2 = -\frac{1}{T}(\mu_1 - \mu_2)\dot{x}. \qquad (81)$$

In the general case, the two mechanisms (75) and (81) operate simultaneously but not additively, since cross terms appear on account of the influence of the nonequilibrium nature of the velocity field. Despite this, (81) enables us to estimate the excess entropy associated with the finite transformation time, which we compare with the total entropy.

We use the same model as in the preceding section. Figure 14 shows the time evolution of the total and the excess entropy $\hat{s}_2$ for the typical initial energy $E/A = 7$ GeV and for relaxation times $\tau = 1$ and 0.1 F/sec. At these energies, a stable shock front is formed. The greater part of the entropy arises during the compression stage as the shock wave passes through the fluid. After this, additional entropy can be formed only in a phase transition. In the expansion stage, the entropy increases by only about 7%. Much the same value was found for expanding quark bubbles with zero baryon charge.[58] Figure 15 shows the entropy as a function of the

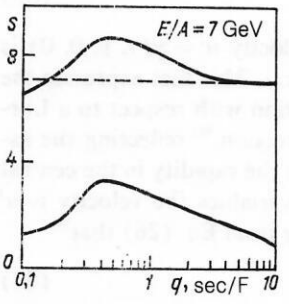

FIG. 15. The produced entropy as a function of the relaxation time $\tau = 1/q$. (The upper curve is the total entropy, and the lower curve is the excess entropy. The broken line is the entropy for an instantaneous phase transition.)

relaxation time. Maxima of both the total and the additional entropy occur near the value $\tau = 0.5$ F/sec. It is worth noting that the difference between the values of the total and the additional entropies depend on the transition time, this indicating the influence of the phase transition on the dynamics of the process. For small τ, the entropy is close to the value obtained from the shock-wave model. For all values of the energy E/A between 5 and 10 GeV, the maximal increase of the entropy is ~ 1.5. An excess of the entropy when the system decays could be a possible signal of a phase transition to a short-lived state of a quark–gluon plasma.

6. ULTRARELATIVISTIC HEAVY-ION COLLISIONS

In accordance with Landau's idea of a growth of the longitudinal distances (see Ref. 89) after a collision with a target nucleon, the high-energy nucleon requires a certain time and distance to be materialized. Owing to the effect of the relativistic increase of the formation time, this distance increases with increasing energy. In the spatial (rapidity) interval between the target and the incident particle, secondary products, mainly pions, appear. The total baryon charge remains in the region of rapidities of the target nucleus and the incident nucleus, whereas in the central region of rapidities the meson density is approximately homogeneous and the baryon density is almost zero. This picture of individual nucleon–nucleon collisions was applied to the description of ultrarelativistic heavy-ion collisions in Ref. 91. An important aspect of this approach is the assumption of penetrability ("transparency") of the nucleus and materialization of particles with zero total baryon charge between the separating highly excited nuclei.

Central region of rapidities

Bjorken hydrodynamics

In Refs. 52, 90, and 92 it was estimated that the particle density is sufficiently high for hydrodynamics to be valid. We consider the longitudinal expansion of the system (the effects of the transverse expansion are discussed in Refs. 52, 53, 58, and 70). The equations of motion (4) are considered in a system of coordinates with line element (light-cone coordinates)

$$ds^2 = -d\tau^2 + \tau^2 d\eta^2 + dy^2 + dz^2, \tag{82}$$

where the Minkowski coordinates are obtained by the inverse transformation

$$t = \tau \cosh \eta;\ x = \tau \sinh \eta. \tag{83}$$

It is assumed that the initial velocity $u^i = \gamma(1, v, 0, 0)$ is determined by the relation $v = x/t$. This fact expresses the invariance of the initial distribution with respect to a Lorentz transformation in the x direction,[90] reflecting the assumed invariance with respect to the rapidity in the central region. Then in the light-cone variables the velocity is $u^i = (1, 0, 0, 0)$. It follows directly from Eq. (26) that[90]

$$\frac{de}{d\tau} + (e + P)/\tau = 0. \tag{84}$$

This equation determines the longitudinal expansion of the system. The dissipative effects are taken into account in Ref. 43.[1)]

Equilibrium confinement

For a relativistic gas of gluons and massless quarks with equation of state $P = -B + (37\pi^2/90)T^4$ the solution of Eq. (84) can be expressed as

$$T = T_0 (\tau_0/\tau)^{1/3},\ \tau s = \text{const}. \tag{85}$$

Assuming that the plasma is transformed into a purely pionic state $[P = (\pi^2/30)T^4]$, the equilibrium transition at $T = T_c$ occurs in a time

$$\tau_f - \tau_0 = \frac{34}{3}\tau_0 (T_0/T_c)^3, \tag{86}$$

where T_0 is the initial temperature, and τ_0 is the time at which the dynamical expansion begins. Equations (85) and (86) mean that the plasma remains for a large fraction of the time in the mixed phase, whereas the pure plasma stage is comparatively short. Since in an equilibrium mixture the velocity of sound is zero, transverse rarefaction cannot penetrate into the system and disturb the longitudinal motion. Therefore, the majority of the signs of the plasma state relate to the transition stage.

Delayed transition to the confinement state

The time of transition to confinement increases in the case of a nonequilibrium phase transition. We first consider a simple transition model for $T = \text{const}$. Equation (84) leads to

$$\tau_f = \tau_i \left(\frac{e_1 - B}{e_2}\right)^{\varepsilon};\quad \varepsilon = \frac{4(e_1 - e_2 - B)}{3(e_1 - e_2)}, \tag{87}$$

where τ_i and τ_f are the times of the beginning and end of the transition. The increase of the entropy in the comoving volume element is

$$\xi \equiv \frac{s_f}{s_i}\Big|_{\text{c.v}} = \frac{s_2\tau_f}{s_1\tau_i} = \frac{e_2}{e_1 - B}\left(\frac{e_1 - B}{e_2}\right)^{\varepsilon}. \tag{88}$$

It can be seen from these equations that a 20% supercooling of the system leads to an increase of the entropy by 2.5 times and a lengthening of the transition time from $\tau_f \sim 12\tau_i$ to $\tau_f \sim 30\tau_i$.

To clarify the possible effects of the supercooling, we use the relaxation law (55) with

$$\left.\begin{aligned} x_{\text{eq}} &= \frac{e - e_2(T_c)}{e_1(T_c) - e_2(T_c)} \quad \text{for} \quad e \geqslant e_2; \\ x_{\text{eq}} &= 0 \quad \text{for} \quad e < e_2. \end{aligned}\right\} \tag{89}$$

The development of the temperature in time is shown in Fig. 16 for two values of the relaxation time.

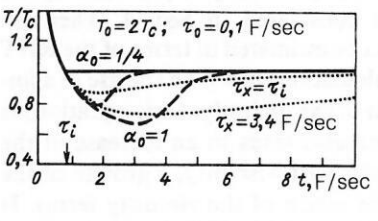

FIG. 16. Evolution of the temperature in the longitudinally expanding central region of rapidities for $x = 0$ and $\tau = t$. The continuous line corresponds to an equilibrium transition, the dotted curves to the relaxation-time approximation (the values of the relaxation time τ_x are given), and the broken curves to classical nucleation theory (the values of the surface-tension parameter α_0 are given).

To compare the results obtained in the relaxation-time approximation with the classical nucleation picture (57), it is necessary to specify the law of the rate of growth of the phase $v(T)$. We choose the form known from the study of materials and which reproduces the limiting cases $v(T_c) = 0$ and $v(0) = 1$:

$$v(T) = 1 - \exp\{k(T - T_c)/T_c\}, \quad k = 6. \tag{90}$$

The results of the comparison are also shown in Fig. 16. It can be seen that in the classical treatment the reheating is much stronger than in the case of the relaxation-time approximation. It is only in the case of a very slow rate of growth that the two models lead to similar results. These examples show that the relaxation-time approximation, which is regarded as one of the simplest realistic models of a nonequilibrium transition, is in this case a good instrument for describing the phenomena under discussion. (However, this approximation is not valid for cosmological transitions.) The surface tension, estimated in Ref. 49 as $\alpha \sim (80\ \text{MeV})^3$, leads to a comparatively small supercooling (of order 5–10%), accompanied by a negligibly small increase of the entropy. Recent investigations[52,53,58] indicate the importance of the effect of the expansion of the system in the transverse direction. The general scheme of numerical solution of the hydrodynamic equations encounters serious difficulties[10] when a complicated equation of state is used. Therefore, the methods mentioned above do not take into account in the equation of state the possibility of a deconfinement phase transition. The approach described in Appendix B makes it possible to apply the method of Lagrangian coordinates described in Appendix A to the description of the charge-symmetric central region of rapidities.

Formation of a baryon-saturated plasma

Since the nuclei pass through each other in ultrarelativistic collisions, they may be compressed and heated. Preliminary estimates of the energy accumulated in a nucleus[85] give hope that the nucleus may undergo a phase transition. This process cannot be described in the framework of a single-fluid model, since the two phases may be different during the time of the complete collision.

Below, we shall use the two-fluid model. If the difference between the rapidities of the target nucleus and the incident nucleus, $\eta - \bar{\eta}$, is sufficiently great that the particles do not succeed in stopping, the baryon charge of either of the two fluids is conserved:

$$(nu^i)_{,i} = (\bar{n}\bar{u}^i)_{,i} = 0. \tag{91}$$

Here, the quantities with the bar correspond to the fluid of the incident nucleus. The particles of the target and the projectile can exchange only energy and momentum. Therefore, Eq. (4) can be generalized to

$$T^{ik}{}_{,k} = F^i; \quad \bar{T}^{ik}{}_{,k} = \bar{F}^i. \tag{92}$$

The force F^i arises because of the coupling between the two fluids and must be calculated by means of the relativistic Boltzmann equation. Approximately, we can obtain[95,96]

$$F^i = -\bar{F}^i = D n \bar{n} (u^i - \bar{u}^i). \tag{93}$$

Owing to the asymmetry with respect to interchange of the velocities u^i and $\bar{u}^i$, the total energy and momentum of the two fluids are conserved. The coefficient D in Eq. (93) can be expressed in terms of the elementary cross sections of particle–particle interaction and the longitudinal momentum transfer[95,96]:

$$D = (\sigma_{\text{el}} \langle p_\parallel \rangle_{\text{el}} + \sigma_{\text{inel}} \langle p_\parallel \rangle_{\text{inel}}). \tag{94}$$

Using on the one hand the elastic part given in Ref. 96 and estimating the contributions of the inelastic interaction as $\langle p_\parallel \rangle_{\text{inel}} = m_t \langle n_\pi \rangle / \eta$, where $\langle n_\pi \rangle$ is the number of created pions with transverse mass $m_t = 0.4$ GeV, we obtain the coefficient D as a smoothly increasing function of the energy which reaches the value $D = 2.5\ \text{GeV}\cdot\text{F}^2$ in the ultrarelativistic limit. On the other hand, analysis of the data on the stopping power of protons with energy 100 GeV leads to the value $D = 1.2\ \text{GeV}\cdot\text{F}^2$.

Equation (94) does not take into account the energy stored in the baryonless plasma that is formed between the separating nuclei at collision energies $E/A > 50$ GeV. To take into account such processes phenomenologically, we can introduce the additional term

$$\tilde{F}^i = \tilde{D}(u^i - w^i), \tag{95}$$

where w^i is the mean velocity of the two fluids, determined by the mean rapidity $\eta_w = (\eta + \bar{\eta})/2$. In the general case, $\tilde{D}$ is not a local function.

Figure 17 shows the results of a calculation with $D = 1.2\ \text{GeV}\cdot\text{F}^2$ obtained in the "layer-on-layer" geometry introduced in Sec. 5 for energies E/A equal to 40 and 160 GeV. Under the assumption of a rapid process of transformation ($\tau = 0.1$ F/sec) the matter reaches a maximal compression exceeding 4 and 6 times, respectively, the normal density in nuclei; moreover, almost all the matter is transformed into the quark phase. The values of the calculated densities are appreciably less than those predicted in single-fluid calculations (for comparison, see Fig. 12). For a long relaxation time ($\tau = 1$ F/sec) the matter is compressed much more strongly, but at the time of greatest compression only a small fraction of the matter (about 25%) is subjected to a phase transition. During the time of the stage of expansion and cooling following the compression stage, the superheated matter changes continuously, and at comparatively

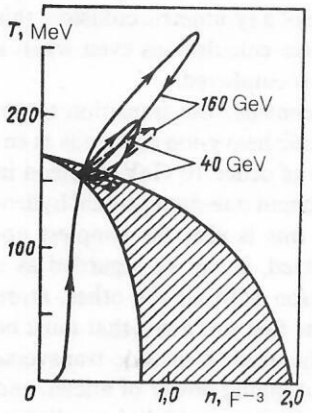

FIG. 17. Trajectories of the state of the matter at the center of a heavy target crossed by an ultrarelativistic nucleus at two collision energies. The continuous curves correspond to $\tau = 1$ F/sec, and the broken curves to $\tau = 0.1$ F/sec; the region of phase coexistence is hatched.

low densities (of order $2.5n_0$) a state close to the state of pure quark matter is reached. In the further development the hadronization stage commences, this occurring as in the single-fluid model. Our hydrodynamic estimates lead to a somewhat higher energy density than the estimates based on study of the production and absorption of secondary particles.[85] During the time of existence of the plasma state, color-neutral particles like photons or leptons can undergo scattering and leave the reaction region. In Appendix C, we describe a method suitable for estimating the flux of particles leaving the system. This scheme was already used in connection with the problem of pion emission in relativistic heavy-ion collisions at not too high energies.

7. CONCLUSIONS

In this paper, we have considered the collision of heavy ions at relativistic energies by hydrodynamic methods. We have demonstrated that these methods in combination with thermodynamics are very suitable for describing collective effects like phase transitions. In the framework of this approach, we have paid particular attention to the deconfinement phase transition, which leads to the formation of a quark–gluon plasma.

Relativistic hydrodynamics is a well-established theory whose formalism is based on conservation of the local energy, momentum, and baryon charge. The general foundations of hydrodynamics and its relationship to kinetic theory were discussed before it was applied to relativistic heavy-ion collisions. It must, however, be remembered that the extension of hydrodynamic methods to such collisions is an idealization of the physical situation. Because a nuclear system is small, significant fluctuations in individual collisions are expected; there can be deviations from local equilibrium due to kinetic effects; and the ignored effects of anisotropy, finite size of the system, and surface effects may compete with the influence of the bulk properties of matter.

We have demonstrated the great flexibility of the hydrodynamic methods. By means of the equation of state, one can consider very different media; the transport coefficients take into account the deviation from equilibrium; the multicomponent formalism enables one to understand the passage of one nucleus through the other; and sink terms describe the fluxes of particles out of the reaction region.

We have presented a new scheme for solving the hydrodynamic equations for the case of a symmetric collision; this is very convenient for computer calculations even when a complicated equation of state is employed.

Our main problem is to consider the transition to deconfinement in central relativistic heavy-ion collisions at energies in the laboratory frame of order 10 GeV/nucleon in the framework of single-component one-dimensional hydrodynamics. It is obvious that this is also the simplest approach. Since it is easily realized, it can be regarded as a suitable scenario for comparison with all the other, more refined approaches. Among the first problems that must be attacked, we must mention the need to include transverse fluxes, transparency, and the stopping power of nuclei, and also the study of asymmetric collisions and full three-dimensional hydrodynamics. With regard to these important effects, the predicted threshold energies for the excitation of quark–gluon degrees of freedom in nuclear matter must be regarded as lower bounds, which are, moreover, insufficiently well determined, owing to our lack of knowledge of the detailed behavior of the equation of state (particularly the bag constant and the coefficient of nuclear compressibility). But even with these shortcomings our results indicate the need to take into consideration the dynamics of the deconfinement phase transition. All calculations that use only the static properties of one phase can at best only predict that a crossing of the phase boundary line does indeed occur under certain conditions, but they are not able to predict what happens to the matter or what is the nature of the dynamical feedback.

In the dynamical approach, we have investigated a delayed deconfinement transition and the idealization of a shock front. Some general results relate to the plasma lifetime, the temperature, density, and entropy, the degree of homogeneity, and the flow pattern. The prediction of the escape of hadrons from the plasma[59,98] is outside the field of applicability of hydrodynamics. Our list of signals indicating the occurrence of a plasma includes a change of the collective flow, an enhancement of fluctuations correlated with an increase of the entropy due to the effects of bubble growth, and (for particular equations of state) the appearance of a double shock wave.

For completeness of the exposition, we list below the signals by means of which a plasma may be distinguished from an ordinary nuclear fireball:

a) Entropy: Owing to the large number of excited degrees of freedom, the entropy in the plasma is appreciably higher,[57] and a nonequilibrium phase transition increases the entropy still further.[91]

b) Collective flow: A phase transition has a strong influence on the flow.[61,97]

c) Spectra of photons and lepton pairs: The rate of formation and the shape of the spectra in the plasma are different from those in the case of a nuclear fireball.[100]

d) Hadron yields: Of particular interest here are strange particles and strange antiparticles, and also antinuclei formed with large probability in the plasma.[59,98]

e) Fluctuations: The kinetics of the "bubbles" in the course of hadronization may lead to characteristic fluctuations with respect to the rapidities.

f) The p_t distribution: The distribution with respect to the mean transverse momentum as a function of the particle number density must become less steep or flatten and have a plateau, this indicating a phase transition.[99]

g) Pion correlations.[102]

h) Excitation of the residual nuclei.[101]

It appears that at the present time only a combination of different measurements will make it possible to identify a plasma, since each of these signals has a competitor among the background events and in the ordinary nuclear fireball. The existing results offer hope of the possibility of formation of a quark–gluon plasma during relativistic heavy-ion collisions. The hopes are based on the use of hydrodynamic methods, which have proved to be a very helpful tool in describing rather complicated collisions of heavy nuclei already at the energies of the accelerators at Dubna and Berkeley.

Many of the results presented in this review were obtained in collaboration with L. P. Csernai. We are very grateful to him for advice during this collaboration. We also

thank V. D. Toneev for helpful comments made during the preparation of this work.

APPENDIX A: HYDRODYNAMIC EQUATIONS IN A COMOVING COORDINATE SYSTEM

In Secs. 1 and 2, we presented the fundamental equations of hydrodynamics. If the appropriate formalism of Riemannian geometry is used, these equations can be cast in a generally covariant form and are then, therefore, valid in an arbitrary coordinate system. However, to find solutions of these equations it is necessary to select a definite system. There are two obvious candidates.

1. The center-of-mass system of the collision (from which one can go over to the laboratory system by means of a Lorentz transformation). This is an inertial coordinate system, and therefore the metric tensor g_{ik} is the tensor of Minkowski space–time, and all the covariant derivatives become partial derivatives. (If necessary, it is possible to introduce cylindrical or polar coordinates.)

2. Comoving coordinate system. In this case, the velocity field becomes trivial, but the metric tensor is nontrivial, since the flow is not inertial.

In principle, these two coordinate systems cover the same possibilities; nevertheless, from the practical point of view there are certain differences. The comoving system is more suitable, since in it the changes of the variables that characterize the fluid are minimal.

We choose a comoving (or Lagrangian) coordinate system and restrict ourselves to plane-symmetric and spherical configurations, these being standard approximations for high-energy collisions of heavy ions. Details of the formalism will be published elsewhere,[84] and here we merely mention the most important aspects for a fluid element for which the irreversibility of the evolution is taken into account only through bulk viscosity.

We consider a single-valued continuous and regular vector field with vector indices u^i. Then there always exists a regular transformation of the coordinates of the type (2) by means of which it is possible to obtain new coordinates:

$$u^i = \delta^i_0. \tag{A.1}$$

The remaining free transformations are

$$x^{0'} = x^0 + f(x^\alpha);\ x^{\alpha'} = x^{\alpha'}(x^\beta);\ \alpha = 1, 2, 3. \tag{A.2}$$

We begin with the line element and the velocity field:

$$\left.\begin{aligned} &ds^2 = -e^{2\varphi}\,dT^2 + e^{2\lambda}\,dY^2 + g_{RS}\,dx^R\,dx^S,\\ &\varphi = \varphi(T, Y),\ \lambda = \lambda(T, Y);\\ &g_{IK} = g_{IK}(T, Y, x^I),\ I = 2, 3;\\ &u^i = (u^T(T, Y),\ u^Y(T, Y),\ 0,\ 0). \end{aligned}\right\} \tag{A.3}$$

This is the case of a plane-symmetric flow, where Y is measured in the direction of the beam, $\varphi = \lambda = 0, g_{22} = g_{33} = 1$, $g_{23} = 0$. Similarly, for the spherical problem, for which Y is the radial coordinate, $\varphi = \lambda = 0, g_{22} = Y^2, g_{33} = Y^2 \sin^2\theta$, $g_{23} = 0$. Then the motion of the particles can be described parametrically as

$$T = T(t, r);\ Y = Y(t, r);\ x^A = x_0^A = \text{const}, \tag{A.4}$$

where r and x^A denote individual particles or mass elements, while t characterizes the evolution of the system. Using t, r, and x_0^A as new coordinates, we obtain[84]

$$\left.\begin{aligned} &ds^2 = -e^{-2\Phi}\,dt^2 + e^{2\Lambda}\,dr^2 + g_{RS}\,dx^R\,dx^S;\\ &\Lambda = \Lambda(t, r),\ \Phi = \Phi(t, r);\\ &u^i = (e^{-\Phi}, 0, 0, 0). \end{aligned}\right\} \tag{A.5}$$

This form is conserved under the transformations

$$\tilde{t} = \tilde{t}(t);\ \tilde{r} = \tilde{r}(r);\ \tilde{x}^A = \tilde{x}^A(x^B). \tag{A.6}$$

Thus, the velocity field becomes trivial, since the unknown functions occur in the geometry. The angle terms in ds^2 take the form

$$g_{RS}dx^R dx^S = \tilde{Y}^2(t, r)\,(d\theta^2 + \Sigma^2(\theta)\,d\varphi^2). \tag{A.7}$$

For spherical symmetry $\Sigma(\theta) = \sin\theta$, whereas for the plane-symmetric case $\Sigma(\theta) = \theta$ and $\tilde{Y} = 1$. In this coordinate system, the hydrodynamic equations (25)–(27) can be rewritten in the form

$$\dot{W} - P\dot{n}/n^2 = 0;\ \Phi' = P'/(e+P);\ n = N_0 B e^{-\Lambda}\tilde{Y}^{-2}. \tag{A.8}$$

Here, the dot denotes the derivatives with respect to the time, and the comma the derivatives with respect to r; N_0 is a constant of integration; $B = 1/4\pi$ for spherical symmetry and $1/F$ for plane symmetry (F is the surface of the model nucleus); finally, W is the specific energy in units of the nucleon rest energy. If there exists a bulk viscosity, then P must be replaced by $\tilde{P}$:

$$\tilde{P} = P - \zeta u^i{}_{;i}, \tag{A.9}$$

where ζ is the coefficient of bulk viscosity. There are further equations which reflect the fact that the metric (A.5) is flat, i.e., equivalent to Eq. (1). Using these equations in conjunction with (A.8) for the new variables u and Γ, which are defined in the spherical case as

$$u = e^{-\Phi}\dot{\tilde{Y}};\ \Gamma = e^{-\Lambda}\tilde{Y}', \tag{A.10}$$

we can obtain the relations

$$e^{-\Phi}\dot{u} = -4\pi\Gamma\tilde{Y}^2\tilde{P}'/\tilde{w};\ \ \Gamma = \sqrt{1+u^2}. \tag{A.11}$$

Here, $\tilde{w}$ is the dimensionless enthalpy:

$$\tilde{w} = (e + \tilde{P})/m_n n \tag{A.12}$$

with

$$u\Phi' e^{\Phi} = \dot{\Gamma} e^{\Lambda}. \tag{A.13}$$

The particle density can be readily found from (A.8) by rewriting it in the form

$$n = \frac{1}{4\pi}\frac{\Gamma N_0}{\tilde{Y}^2\tilde{Y}'}. \tag{A.14}$$

For the plane-symmetric case, one can use Eq. (A.4) for the coordinate Y instead of $\tilde{Y}$ and again obtain, by the substitution $4\pi\tilde{Y}^2 \to F$, the first equation of (A.11) together with the relation

$$u' e^{\Phi} = \dot{e}^{\Lambda}\Gamma \tag{A.15}$$

and, thus, again have Eqs. (A.13) and (A.14).

The present equations can be solved by means of the difference scheme described in detail in Refs. 71 and 84. It is important to note that the evolution equations in the Lagrangian coordinates admit appropriate weighting of all quantities. Then the structure of the equations has the form $\{A(t + \Delta t)\} = \{B(t)\}$ with $\{A\} = (u, Y)$, and $\{B(t)\}$ can be calculated directly from $\{A(t)\}$ by means of the remain-

ing algebraic equations. Other schemes used to solve the hydrodynamic equations are based on the use of mixed Eulerian and Lagrangian coordinates (see Refs. 93 and 94); in the case of complicated equations of state they require much computing time.

APPENDIX B: CHARGE-SYMMETRIC CASE

The formalism presented in Appendix A uses the particle densities in explicit form, and therefore it cannot be directly used in the cases when the thermodynamic description does not contain particle degrees of freedom, i.e., when there is no conservation of particles except, perhaps, a charge-symmetric mixture of particles and antiparticles. One of these very important cases is the central region of rapidities in high-energy nucleus–nucleus collisions.[85]

Since the possibility of hydrodynamic description of this region is very attractive,[90] it is necessary to extend the formalism in such a way as to include in it this situation as well. This can be readily done in the absence of irreversibility, when the entropy is a conserved quantity:

$$(su^i)_{;i} = 0. \tag{B.1}$$

Then instead of the special system with thermodynamic potential

$$s = s(e) \tag{B.2}$$

(where s is the entropy density), we can define a new system as

$$\tilde{e} = e;\ n = Cs;\ \tilde{s} = \tilde{s}(\tilde{n}, \tilde{e}) = s(e)\,\chi(n/s). \tag{B.3}$$

If C is a dimensionless constant, then the dynamical behavior of this new system remains the same as before ($\tilde{P} = P$).[87] Here, χ is an arbitrary (positive) function whose actual value is taken to be constant by virtue of the second equation in (B.3).

Thus, one introduces a "spurious" particle, which is conserved in accordance with (B.1). In the general case, this spurious number is not equal to the number of real particles, except for particles of negligibly small mass.[87]

APPENDIX C: SINK TERMS

In some stages of the expansion of the system there may be direct emission of particles. In this case, strictly speaking, there is no well-defined velocity field in the matter, so that the hydrodynamic formalism is not fully justified. Despite this, such bulk emission can sometimes be simulated by means of nonconserved terms. We first consider a single-component system, dividing it into two subsystems: particles that remain in the given (expanding) volume and particles that leave the system. Since neither the particle flux nor the energy–momentum tensor of the first subsystem is conserved, we can write

$$(nu^i)_{;i} = -qn, \tag{C.1}$$

where q is the rate of loss of particles, a constant quantity in the simplest model.

Further, for T^{ij} there also exists a vector loss term. Assuming that each emitted particle carries away with it certain mean values of the momentum and energy, we can obtain

$$T^{ij}_{;j} = -qT^{ij}u_j \tag{C.2}$$

(details are given in Ref. 84). After this, rewriting the hydrodynamic equations (23) and (24), we can obtain modified balance equations for the particles and the energy:

$$\dot{n} + n^r{}_{;r} = -qn;\ \dot{\varepsilon} + (\varepsilon + P)\,u^r{}_{;r} = -q\varepsilon. \tag{C.3}$$

The equation for the acceleration is unchanged (here, the dot represents $u^r\nabla_r$). After this, one can again introduce a bulk viscosity and repeat the calculations of Appendix A.

Because the velocity field does not have a unique value, Lagrangian coordinates are inconvenient for describing the baryon loss. For nonbaryon losses, this problem does not exist. For further discussions, see Ref. 88.

[1)] Bjorken's original paper[90] corresponds to zero baryon density in the central region of rapidities, i.e., $n = 0$. However, recent investigations[67] have shown that baryon charge is dispersed over the complete region of rapidities. In this case, the baryon density is determined by the continuity equation (27) as $\tau n = \text{const}$.

[1] D. Iwanenko and D. E. Kurtgelaidze, Lett. Nuovo Cimento **2**, 13 (1969); N. Itoh, Prog. Theor. Phys. **44**, 291 (1970).
[2] J. C. Collins and M. J. Perry, Phys. Rev. Lett. **34**, 1353 (1975); G. Chapline and M. Nauenberg, Phys. Rev. D **16**, 450 (1977); G. Baym and S. A. Chin, Phys. Lett. **62B**, 241 (1976); B. D. Keister and L. S. Kisslinger, Phys. Lett. **64B**, 117 (1976); B. A. Freedman and L. McLerran, Phys. Rev. D **16**, 1130, 1147 (1977); **17**, 1109 (1978).
[3] A. S. Chin, Phys. Lett. **78B**, 552 (1978).
[4] G. Chapline and A. Kerman, Laurence Livermore Laboratory Report UCRL-80737 (1978).
[5] J. Kapusta, Nucl. Phys. **148**, 461 (1979).
[6] D. K. Kalashnikov and V. V. Klimov, Phys. Lett. **88B**, 328 (1979).
[7] E. V. Shuryak, Phys. Rep. **61**, 71 (1980).
[8] H. Stöcker, G. Graebner, J. A. Maruhn, and W. Greiner, Z. Phys. A **295**, 401 (1980).
[9] H. Stöcker, G. Graebner, J. A. Maruhn, and W. Greiner, Phys. Lett. **95B**, 192 (1980).
[10] H. Stöcker and W. Greiner, Phys. Rep. **137**, 277 (1986); D. Strottman and R. B. Clare, Phys. Rep. **141**, 177 (1986).
[11] S. Z. Belen'kiĭ and L. D. Landau, Usp. Fiz. Nauk **56**, 309 (1955); Nuovo Cimento Suppl. **3**, 15 (1956); L. D. Landau, Izv. Akad. Nauk SSSR **17**, 51 (1953).
[12] *Quark Matter 84* (Lecture Notes in Physics, Vol. 221), edited by K. Kajantie (Springer Verlag, Berlin, 1985); J. Cleymans, R. V. Gavai, and E. Suhonen, Phys. Rep. **130**, 217 (1986).
[13] B. Müller, *The Physics of the Quark–Gluon Plasma* (Lecture Notes in Physics, Vol. 225) (Springer, Berlin, 1985).
[14] M. Jacob and J. Tran Thanh Van (editors), Phys. Rep. **88**, 321 (1982).
[15] L. D. Landau and E. M. Lifshitz, *Fluid Mechanics*, 2nd ed. (Pergamon Press, Oxford, 1987) [Russ. original, Nauka, Moscow, 1953].
[16] C. W. Misner, K. S. Thorn, and J. A. Wheeler, *Gravitation* (Wiley, San Francisco, 1982) [Russ. transl., Mir, Moscow, 1977, Vols. 1–3).
[17] L. P. Csernai and B. Lukacs, Acta Phys. Pol. **B15**, 149 (1984).
[18] A. H. Taub, *Relativity Theory and Astrophysics*, Vol. 1, edited by J. Ehlers (American Mathematical Society, Providence, R. I., 1967).
[19] N. A. Chernikov, Dokl. Akad. Nauk SSSR **112**, 1030 (1957); **114**, 530 (1957) [Sov. Phys. Dokl. **2**, 248 (1958)]; Acta Phys. Pol. **23**, 629 (1963); Phys. Lett. **5**, 115 (1963).
[20] J. Ehlers, in: *Proc. of the Intern. School "Enrico Fermi"*, Vol. 47 (1971), p. 1; in: *Relativity, Astrophysics and Cosmology*, edited by W. Israel (Reidel, Dordrecht, 1973), p. 1.
[21] H. Grad, *Handbuch der Physik XII. Theorie der Gase*, edited by S. Flügge (Springer, Berlin, 1967).
[22] B. Lukács, K. Martinás, and T. Pacher, Astron. Nachr. **307**, 171 (1986).
[23] B. Lukács and K. Martinás, KFKI-Budapest Report, KFKI-1984-25, p. 24.
[24] A. I. Akhiezer and S. V. Peletminskiĭ, *Methods of Statistical Physics* (Pergamon Press, Oxford, 1981) [Russ. original, Nauka, Moscow, 1977].
[25] G. S. Hall and J. Arab, Sci. Eng. **9**, 87 (1984).
[26] T. M. Reed and K. E. Gubbins, *Applied Statistical Mechanics. Thermo-*

dynamics and Transport Properties of Fluids (McGraw-Hill, New York, 1972).
[27]P. T. Landsberg, *Thermodynamics* (Interscience, New York, 1961); H. B. Callen, *Thermodynamics* (Wiley, New York, 1960).
[28]B. D. Day, Rev. Mod. Phys. **50**, 495 (1978).
[29]M. G. Barranco and J. R. Buchler, Phys. Rev. C **22**, 1729 (1980); **24**, 1191 (1981); G. Röpke, L. Münchow, and H. Schulz, Nucl. Phys. **A379**, 536 (1982); Phys. Lett. **110B**, 21 (1982).
[30]B. Friedman and V. R. Pandharipande, Nucl. Phys. **A361**, 502 (1981); B. Friedman, V. R. Pandharipande, and Q. N. Usmani, Nucl. Phys. **A372**, 483 (1981).
[31]J. D. Walecka, Ann. Phys. (N.Y.) **83**, 491 (1974); Phys. Lett. **59B**, 109 (1975); J. Boguta and A. R. Bodmer, Nucl. Phys. **A292**, 413 (1971).
[32]H. Reinhard and H. Schulz, Nucl. Phys. **A432**, 630 (1985).
[33]T. Celik, J. Engels, and H. Satz, Phys. Lett. **129B**, 323 (1983); F. Fucito and S. Solomon, Phys. Lett. **149B**, 387 (1984); J. Polonyi *et al.*, Phys. Rev. Lett. **53**, 644 (1984).
[34]J. W. Harris, R. K. Bock, R. Brockmann *et al.*, Phys. Lett. **153B**, 377 (1985); R. Stock, R. Bock, R. Brockmann *et al.*, Phys. Rev. Lett. **49B**, 1236 (1982).
[35]M. Sano, M. Gyulassy, M. Wakai, and Y. Kitazoe, Phys. Lett. **156B**, 27 (1985).
[36]P. Hasenfratz, R. R. Horgan, J. Kuti, and J. M. Richard, Phys. Lett. **94B**, 401 (1980).
[37]C. G. Kälman, Phys. Lett. **134B**, 363 (1984).
[38]S. R. De Groot and P. Mazur, *Non-Equilibrium Thermodynamics* (North-Holland, Amsterdam, 1962).
[39]G. Neugebauer, *Relativistische Thermodynamik* (Akademie-Verlag, Berlin, 1980).
[40]W. A. Hiscock and L. Lindblom, Ann. Phys. (N.Y.) **151**, 466 (1983); W. Israel and J. M. Stewart, Ann. Phys. (N.Y.) **118**, 341 (1979).
[41]G. Buchwald, L. Csernai, J. A. Maruhn *et al.*, Phys. Rev. C **24**, 135 (1981).
[42]P. Danielewics, Phys. Lett. **146B**, 168 (1984).
[43]P. Danielewics and M. Gyulassy, Phys. Rev. D **31**, 53 (1985); A. Hosaya and K. Kajantie, Nucl. Phys. **B250**, 666 (1985).
[44]I. Montvay and J. Zimanyi, Nucl. Phys. **A316**, 490 (1979).
[45]L. P. Csernai and B. Lukács, Phys. Lett. **132B**, 295 (1983).
[46]*Nucleation Phenomena*, edited by A. C. Zettelmoyer (Elsevier, Amsterdam, 1977).
[47]L. D. Landau and E. M. Lifshitz, *Statistical Physics*, 2nd ed. (Pergamon Press, Oxford, 1969) [Russ. original, Nauka, Moscow, 1964].
[48]A. D. Linde, Nucl. Phys. **B216**, 421 (1983); S. Coleman, Phys. Rev. D **15**, 2929 (1977).
[49]H. Reinhardt and B. V. Dang, Phys. Lett. **173**, 473 (1986); E. Fahri and R. L. Jaffe, Phys. Rev. D **30**, 2379 (1984).
[50]P. Steinhardt, Phys. Rev. D **25**, 2074 (1982).
[51]M. Gyulassy, K. Kajantie, H. Kurki-Suonio, and L. McLerran, Nucl. Phys. **B237**, 477 (1984).
[52]G. Baym, B. L. Friman, J. P. Bloizot *et al.*, Nucl. Phys. **A407**, 541 (1983).
[53]N. K. Glendenning and T. Matsui, Phys. Lett. **141B**, 419 (1984).
[54]Z. P. Csernai, Phys. Rev. D **29**, 1945 (1984).
[55]B. Kämpfe, J. Phys. G **9**, 1487 (1983).
[56]H. Stöcker, Nucl. Phys. **A418**, 587 (1984).
[57]B. L. Friman, G. Baym, and J. P. Blaizot, Phys. Lett. **132B**, 291 (1983).
[58]G. E. Duvall and R. A. Graham, Rev. Mod. Phys. **49**, 523 (1977).
[59]B. Kämpfer, H. W. Barz, L. Münchow, and B. Lukács, Acta Phys. Pol. **B17**, 685 (1986).
[60]A. Taub, Phys. Rev. **74**, 328 (1948).
[61]H. W. Barz, L. P. Csernai, B. Kämpfer, and B. Lukács, Phys. Rev. D **32**, 115 (1985).
[62]Ya. B. Zel'dovich and Yu. P. Raizer, *Physics of Shock Waves and High-Temperature Hydrodynamic Phenomena*, Vols. 1 and 2 (Scripta Technica, New York, 1966, 1967) [Russ. original, Nauka, Moscow, 1966].
[63]V. M. Galitskij and I. N. Mishustin, Phys. Lett. **72B**, 285 (1978).
[64]G. Graebner, Thesis, University of Frankfurt/Main (1985), p. 112.
[65]M. Gyulassy, Nucl. Phys. **A400**, 31 (1983); in: *Proc. of the Intern. Conf. on High Energy Physics* (Balatonfüred, Hungary, 1983), p. 489.
[66]D. S. Barton, G. W. Brandenburg, W. Busza *et al.*, Phys. Rev. D **27**, 2580 (1983); W. Busza and A. S. Goldhaber, Phys. Lett. **139B**, 235 (1984); R. C. Hwa, Phys. Rev. Lett. **52**, 492 (1984); L. P. Csernai and J. Kapusta, Phys. Rev. D **29**, 2664 (1984); **31**, 2795 (1985); K. Hüfner and A. Klar, Phys. Lett. **145B**, 167 (1984).
[67]S. Daté, M. Gyulassy, and H. Sumiyoshi, Phys. Rev. D **32**, 619 (1985).
[68]H. Bethe, "Theory of shock waves for an arbitrary equation of state," Office of Scientific Research and Development Report, No. 545 (1942).
[69]G. F. Chapline, in: *Proc. of the Seventh High-Energy Heavy Ion Study* (GSI Darmstadt, Oct., 1984, GSI-85-10, 1985), p. 45.
[70]R. C. Hwa, Phys. Rev. D **32**, 637 (1985).
[71]K. A. Van Riper, Astrophys. J. **232**, 558 (1979).
[72]H. Reinhardt, B. V. Dang, and H. Schulz, Phys. Lett. **159B**, 161 (1986); J. Kuti, B. Lukács, J. Polonyi, and K. Szachanyi, Phys. Lett. **95B**, 75 (1980); M. I. Gorenstein, S. I. Lipskikh, and G. M. Zinovjev, Z. Phys. C **22**, 189 (1984); E. M. Ilgenfritz and L. Kripfganz, Z. Phys. C **29**, 77 (1985); D. Blaschke, F. Reinholz, G. Röpke, and D. Kremp, Phys. Lett. **151B**, 439 (1985); R. Kämpfer, H. Schulz, and C. J. Horowitz, Ann. Phys. (N.Y.) **41**, 291 (1984); R. Hagedorn and J. Rafelski, Phys. Lett. **97B**, 136 (1980).
[73]T. S. Biro and J. Zimányi, Nucl. Phys. **A395**, 525 (1983).
[74]J. Randrup, Nucl. Phys. **A314**, 429 (1979).
[75]G. Bertsch and J. Cugnon, Phys. Rev. C **24**, 2514 (1981).
[76]K. K. Gudima, V. D. Toneev, G. Röpke, and H. Schulz, Phys. Rev. C **32**, 1605 (1985).
[77]H. Stöcker, J. Phys. G **10**, L111 (1984).
[78]P. J. Siemens and J. I. Kapusta, Phys. Rev. Lett. **43**, 1486 (1979).
[79]T. Biro, H. W. Barz, B. Lukács, and J. Zimányi, KFKI Budapest Report KFKI-90 (1984), p. 18.
[80]H. Sato and K. Tazaki, Phys. Lett. **98B**, 153 (1981).
[81]G. Röpke, M. Schmidt, L. Münchow, and H. Schulz, Nucl. Phys. **A399**, 587 (1983).
[82]L. P. Czernai, Phys. Rev. Lett. **54**, 639 (1985).
[83]L. P. Csernai and H. W. Barz, Z. Phys. **A296**, 173 (1980).
[84]B. Kämpfer and B. Lukács, Acta Phys. Hung. **61**, 151 (1986).
[85]R. Anishetty, P. Kohler, and L. McLerran, Phys. Rev. D **22**, 2793 (1983).
[86]J. B. Kogut, Y. Matsuoka, M. Stone *et al.*, Phys. Rev. Lett. **51**, 869 (1983); J. B. Kogut and D. K. Sinclair, University of Illinois Preprint ILL-(TH)-8-46, p. 43.
[87]B. Lukács and K. Martinás, Acta Phys. Slovaca **36**, 86 (1986).
[88]H. W. Barz, L. P. Csernai, and W. Greiner, Phys. Rev. C **26**, 740 (1982).
[89]N. N. Nikolaev, Fiz. Elem. Chastits At. Yadra **12**, 162 (1981) [Sov. J. Part. Nucl. **12**, 63 (1981)].
[90]J. D. Bjorken, Phys. Rev. D **27**, 140 (1983).
[91]H. W. Barz, B. Kämpfer, B. Lukács, and L. P. Csernai, Phys. Rev. C **31**, 268 (1985).
[92]G. Baym, Phys. Lett. **138B**, 18 (1984); K. Kajantie and T. Matsui, Phys. Lett. **164B**, 373 (1985).
[93]F. Harlow, A. A. Amsden, and J. R. Nix, J. Comput. Phys. **20**, 119 (1976).
[94]A. S. Roshal' and V. N. Russkikh, Yad. Fiz. **33**, 1520 (1981) [Sov. J. Nucl. Phys. **33**, 817 (1981)].
[95]A. Amsden, A. Goldhaber, F. Harlow, and J. Nix, Phys. Rev. C **17**, 2080 (1977).
Y. Ivanov, I. Mishustin, and L. Satarov, Nucl. Phys. **A433**, 713 (1985).
[97]B. Kämpfer, H. W. Barz, and L. P. Csernai, UMTNP-115 (1984), p. 17.
[98]P. Koch, B. Müller, and J. Rafelski, Phys. Rep. **142**, 169 (1986); U. Heinz, P. R. Subramanian, and W. Greiner, Z. Phys. A **318**, 247 (1984).
[99]L. Van Hove, Phys. Lett. **118B**, 138 (1982); B. Friman, K. Kajantie, and P. V. Ruuskanen, HU-TFT-85-21, p. 37.
[100]G. Domokos and J. I. Goldman, Phys. Rev. D **23**, 203 (1981); K. Kajantie and H. I. Miettinen, Z. Phys. C **9**, 341 (1981); S. A. Chin, Phys. Lett. **119B**, 51 (1982).
[101]S. Raha, R. M. Weiner, and J. W. Wheeler, Phys. Rev. Lett. **53**, 138 (1984).
[102]J. A. Lopez, J. C. Parikh, and P. J. Siemens, Phys. Rev. Lett. **53**, 1216 (1984); J. I. Kapusta, Phys. Lett. **134B**, 233 (1984).
[103]B. Kämpfer, H. W. Barz, and B. Lukács, KFKI-Report-85-77, p. 19.
[104]H. W. Barz, B. Kämpfer, L. P. Csernai, and B. Lukács, Phys. Lett. **143B**, 334 (1984).

Translated by Julian B. Barbour